Plasmodium falciparum K13 mutations in Africa and Asia impact artemisinin resistance and parasite fitness

Barbara H. Stokes, Satish K. Dhingra, Kelly Rubiano, Sachel Mok, Judith Straimer, Nina F. Gnadig, Ioanna Deni, Kyra A. Schindler, Jade R. Bath, Kurt E. Ward, et al.

Plasmodium falciparum K13 mutations in Africa and Asia impact artemisinin resistance and parasite fitness

Barbara H. Stokes[1], Satish K. Dhingra[1], Kelly Rubiano[1], Sachel Mok[1], Judith Straimer[1], Nina F. Gnädig[1], Ioanna Deni[1], Kyra A. Schindler[1], Jade R. Bath[1], Kurt E. Ward[1,2], Josefine Striepen[1], Tomas Yeo[1], Leila S. Ross[1], Eric Legrand[3], Frédéric Ariey[4], Clark H. Cunningham[1,5], Issa M. Souleymane[6], Adama Gansané[7], Romaric Nzoumbou-Boko[8], Claudette Ndayikunda[9], Abdunoor M. Kabanywanyi[10], Aline Uwimana[11], Samuel J. Smith[12], Olimatou Kolley[13], Mathieu Ndounga[14], Marian Warsame[15], Rithea Leang[16], François Nosten[17,18], Timothy J.C. Anderson[19], Philip J. Rosenthal[20], Didier Ménard[3], David A. Fidock[1,21‡]

[1]Department of Microbiology and Immunology, Columbia University Irving Medical Center, New York, NY, USA; [2]Department of Microbiology and Immunology, University of Otago, Dunedin, New Zealand; [3] Malaria Genetics and Resistance Unit, Institut Pasteur, INSERM U1201, CNRS ERL9195, Paris, France; [4]Institut Cochin INSERM U1016, Université Paris Descartes, Paris, France; [5]Department of Genetics, University of North Carolina at Chapel Hill, Chapel Hill, NC, USA; [6]Programme National de Lutte Contre le Paludisme au Tchad, Ndjamena, Chad; [7]Centre National de Recherche et de Formation sur le Paludisme, Ouagadougou, Burkina Faso; [8]Laboratory of Parasitology, Institute Pasteur of Bangui, Bangui, Central African Republic; [9]University Teaching Hospital of Kamenge, Bujumbura, Burundi; [10]Ifakara Health Institute, Dar es Salaam, Tanzania; [11]Malaria and Other Parasitic Diseases Division, Rwanda Biomedical Centre, Kigali, Rwanda; [12]National Malaria Control Programme, Sierra Leone; [13]National Malaria Control Program, Banjul, The Gambia; [14]Programme National de Lutte Contre le Paludisme, Brazzaville, République du Congo; [15]School of Public Health and Community Medicine, University of Gothenburg, Sweden; [16]National Center for Parasitology, Entomology & Malaria Control, Phnom Penh, Cambodia; [17]Shoklo Malaria Research Unit, Mahidol-Oxford Tropical Medicine Research Unit, Faculty of Tropical Medicine, Mahidol University, Mae Sot, Thailand; [18]Centre for Tropical Medicine and Global Health, Nuffield Department of Medicine, University of Oxford, Oxford, UK; [19]Texas Biomedical Research Institute, San Antonio, TX, USA; [20]Department of Medicine, University of California, San Francisco, CA, USA; [21]Division of Infectious Diseases, Department of Medicine, Columbia University Irving Medical Center, New York, NY, USA

‡Corresponding author. Email: df2260@cumc.columbia.edu

Abstract

The emergence of mutant K13-mediated artemisinin (ART) resistance in *Plasmodium falciparum* malaria parasites has led to widespread treatment failure across Southeast Asia. In Africa, *K13*-propeller genotyping confirms the emergence of the R561H mutation in Rwanda and highlights the continuing dominance of wild-type K13 elsewhere. Using gene editing, we show that R561H, along with C580Y and M579I, confer elevated *in vitro* ART resistance in some African strains, contrasting with minimal changes in ART susceptibility in others. C580Y and M579I cause substantial fitness costs, which may slow their dissemination in high-transmission settings, in contrast with R561H that in African 3D7 parasites is fitness neutral. In Cambodia, *K13* genotyping highlights the increasing spatio-temporal dominance of C580Y. Editing multiple K13 mutations into a panel of Southeast Asian strains reveals that only the R561H variant yields ART resistance comparable to C580Y. In Asian Dd2 parasites C580Y shows no fitness cost, in contrast with most other K13 mutations tested, including R561H. Editing point mutations in *ferredoxin* or *mdr2*, earlier associated with resistance, has no impact on ART susceptibility or parasite fitness. These data underline the complex interplay between K13 mutations, parasite survival, growth and genetic background in contributing to the spread of ART resistance.

Introduction

Despite recent advances in chemotherapeutics, diagnostics and vector control measures, malaria continues to exert a significant impact on human health (Hanboonkunupakarn and White, 2020). In 2019, cases were estimated at 229 million, resulting in 409,000 fatal outcomes, primarily in Sub-Saharan Africa as a result of *Plasmodium falciparum* infection (WHO, 2020). This situation is predicted to worsen as a result of the ongoing SARS-CoV-2 pandemic that has compromised malaria treatment and prevention measures (Sherrard-Smith *et al.*, 2020). Absent an effective vaccine, malaria control and elimination strategies are critically reliant on the continued clinical efficacy of first-line artemisinin-based combination therapies (ACTs) (White *et al.*, 2014). These ACTs pair fast-acting artemisinin (ART) derivatives with partner drugs such as lumefantrine, amodiaquine, mefloquine or piperaquine (PPQ). ART derivatives can reduce the biomass of drug-sensitive parasites by up to 10,000-fold within 48 h (the duration of one intra-erythrocytic developmental cycle); however, these derivatives are rapidly metabolized *in vivo*. Longer-lasting albeit slower-acting partner drugs are co-administered to reduce the selective pressure for ART resistance and to clear residual parasitemias (Eastman and Fidock, 2009).

P. falciparum resistance to ART derivatives has now swept across Southeast (SE) Asia, having first emerged a decade ago in western Cambodia (Dondorp *et al.*, 2009; Noedl *et al.*, 2009; Ariey *et al.*, 2014; Imwong *et al.*, 2020). Clinically, ART resistance manifests as delayed clearance of circulating asexual blood stage parasites following treatment with an ACT but does not result in treatment failure as long as the partner drug remains effective. The accepted threshold for resistance is a parasite clearance half-life (the time required for the peripheral blood parasite density to decrease by 50%) of >5.5 h. Sensitive parasites are typically cleared in <2-3 h (WHO, 2019). Resistance can also be evidenced as parasite-positive blood smears on day three post initiation of treatment. *In vitro,* ART resistance manifests as an increase in survival in tightly synchronized ring-stage parasites (0-3 h post invasion) exposed to a 6 h pulse of 700 nM dihydroartemisinin (DHA, the active metabolite of all ARTs used clinically) in the ring-stage survival assay (RSA) (Witkowski *et al.*, 2013; Ariey *et al.*, 2014). Recently, ART-resistant strains have also acquired resistance to PPQ, which is widely used in SE Asia as a partner drug in combination with DHA (Wicht *et al.*, 2020). Failure rates following DHA-PPQ treatment now exceed 50% in parts of Cambodia, Thailand and Vietnam (van der Pluijm *et al.*, 2019).

In vitro selections, supported by clinical epidemiological data, have demonstrated that ART resistance is primarily determined by mutations in the beta-propeller domain of the *P. falciparum* Kelch protein K13, also known as Kelch13 (Ariey *et al.*, 2014; Ashley *et al.*, 2014; MalariaGEN, 2016; Menard *et al.*, 2016; Siddiqui *et al.*, 2020). Recent evidence suggests that these mutations result in reduced endocytosis of host-derived hemoglobin and thereby decrease the release of Fe^{2+}-heme that serves to activate ART, thus reducing its potency (Yang *et al.*, 2019; Birnbaum *et al.*, 2020). Mutations in other genes including *ferredoxin (fd)* and *multidrug resistance protein 2 (mdr2)* have also been associated with ART resistance in K13 mutant parasites, leading to the suggestion that they either contribute to a multigenic basis of resistance or fitness or serve as genetic markers of founder populations (Miotto *et al.*, 2015).

In SE Asia, the most prevalent K13 mutation is C580Y, which associates with delayed clearance *in vivo* (Ariey *et al.*, 2014; Ashley *et al.*, 2014; MalariaGEN, 2016; Menard *et al.*, 2016; Imwong *et al.*, 2017). This mutation also mediates ART resistance *in vitro,* as demonstrated by RSAs performed on gene-edited parasites (Ghorbal *et al.*, 2014; Straimer *et al.*, 2015; Straimer *et al.*, 2017; Mathieu *et al.*, 2020; Uwimana *et al.*, 2020). Other studies have documented the emergence of nearly 200 other K13 mutations, both in SE Asia and in other malaria-endemic regions, including the Guiana Shield and the western Pacific (MalariaGEN, 2016; Menard *et al.*, 2016; Das *et al.*, 2019; WWARN, 2019; Mathieu *et al.*, 2020; Miotto *et al.*, 2020). Aside from C580Y, however, only a handful of K13 mutations (N458Y, M476I, Y493H, R539T, I543T and R561H) have been validated by gene-editing experiments as conferring resistance *in vitro* (Straimer *et al.*, 2015; Siddiqui *et al.*, 2020). Nonetheless, multiple other mutations in this gene have been associated with the clinical delayed clearance phenotype and have been proposed as candidate markers of ART resistance (WWARN, 2019; WHO, 2019).

Here, we define the role of a panel of K13 mutations identified in patient isolates, and address the key question of whether these mutations can confer resistance in African strains. We include the K13 R561H mutation, earlier associated with delayed parasite clearance in SE Asia (Ashley *et al.*, 2014; Phyo *et al.*, 2016), and very recently identified at up to 13% prevalence in certain districts in Rwanda (Uwimana *et al.*, 2020; Bergmann *et al.*, 2021; Uwimana *et al.*, 2021). This study also enabled us to assess the impact of the parasite genetic background on *in vitro* phenotypes, including mutations in *ferredoxin* and *mdr2* that were earlier associated with resistance (Miotto

et al., 2015). Our results show that K13 mutations can impart ART resistance across multiple Asian and African strains, at levels that vary widely depending on the mutation and the parasite genetic background. Compared with K13 mutant Asian parasites, we observed stronger *in vitro* fitness costs in most K13-edited African strains, which might predict a slower dissemination of ART resistance in high-transmission African settings. Nonetheless, our data highlight the threat of the R561H mutation emerging in Rwanda, which confers elevated RSA resistance and minimal fitness cost in African 3D7 parasites.

Results

Non-synonymous K13 mutations are present at low frequencies in Africa

To examine the status of K13 mutations across Africa, we analyzed *K13* beta-propeller domain sequences in 3,257 isolates from 11 malaria-endemic African countries, including The Gambia, Sierra Leone, and Burkina Faso in West Africa; Chad, Central African Republic, Republic of the Congo, and Equatorial Guinea in Central Africa; and Burundi, Tanzania, Rwanda, and Somalia in East Africa. Samples were collected between 2012 and 2019, with most countries sampled across multiple years. 1,038 (32%) originated from The Gambia, Republic of the Congo and Burundi and have not been previously reported, whereas the remaining samples including those from Rwanda have been published (**Figure 1–Source data 1; Supplementary file 1**).

Of all samples, 98% (3,179) were K13 wild-type, i.e. they matched the 3D7 (African) reference sequence or harbored a synonymous (non-coding) mutation. For individual countries, the percentage of K13 wild-type samples ranged from 95% to 100% (**Figure 1; Figure 1–source data 1**). In total, we identified 35 unique non-synonymous mutations in K13. Of these, only two have been validated as resistance mediators in the SE Asian Dd2 strain: the M476I mutation initially identified from long-term ART selection studies and the R561H mutation observed in SE Asia and Rwanda (Ariey *et al.*, 2014; Straimer *et al.*, 2015; Uwimana *et al.*, 2020).

Of the 35 non-synonymous mutations, only two were present in >6 samples: R561H (n=20, found only in Rwanda, sampled from 2012 to 2015; (Uwimana *et al.*, 2020)), and A578S (n=10; observed in four African countries across multiple years). Previously A578S was shown not to confer *in vitro* resistance in Dd2 (Menard

et al., 2016). In the set of 927 genotyped Rwandan isolates, R561H accounted for 44% of mutant samples and 2% of all samples (**Figure 1 inset**).

K13 R561H, M579I and C580Y mutations can confer *in vitro* artemisinin resistance in African parasites

To test whether R561H can mediate ART resistance in African strains, we developed a CRISPR/Cas9-mediated *K13* editing strategy (**Supplementary file 2**) to introduce this mutation into 3D7 and F32 parasites. On the basis of whole-genome sequence analysis of African isolates, 3D7 was recently shown to segregate phylogenetically with parasites from Rwanda (Ariey *et al*., 2014; Uwimana *et al*., 2020). F32 was derived from an isolate from Tanzania (Witkowski *et al*., 2010). We also tested the C580Y mutation that predominates in SE Asia, as well as the M579I mutation earlier identified in a *P. falciparum*-infected migrant worker in Equatorial Guinea who displayed delayed parasite clearance following ACT treatment (Lu *et al*., 2017). The positions of these residues are highlighted in the K13 beta-propeller domain structure shown in **Supplementary file 3**. For 3D7, F32 and other lines used herein, their geographic origins and genotypes at drug resistance loci are described in **Table 1** and **Supplementary file 4**. All parental lines were cloned by limiting dilution prior to transfection. Edited parasites were identified by PCR and Sanger sequencing, and cloned. These and other edited parasite lines used herein are described in **Supplementary file 5**.

RSAs, used to measure *in vitro* ART susceptibility, revealed a wide range of mean survival values for K13 mutant lines. For 3D7 parasites, the highest RSA survival rates were observed with $3D7^{R561H}$ parasites, which averaged 6.6% RSA survival. For the $3D7^{M579I}$ and $3D7^{C580Y}$ lines, mean RSA survival rates were both 4.8%, a 3 to 4-fold increase relative to the $3D7^{WT}$ line. No elevated RSA survival was seen in a 3D7 control line ($3D7^{ctrl}$) that expressed only the silent shield mutations used at the guide RNA cut site (**Figure 2A; Figure 2–source data 1**). Western blot analysis with tightly synchronized ring-stage parasites revealed a ~30% reduction in K13 protein expression levels in these three K13 mutant lines relative to the parental $3D7^{WT}$ (**Figure 2–figure supplement 1; Figure 2–figure supplement 1–source data 1**).

Interestingly, for F32 parasites the introduction of K13 mutations yielded no significant increase in RSA survival, whose rates were in the range of 0.3% to 0.5% for lines expressing R561H, M579I, C580Y or wild-type K13. (**Figure 2B**). Previously we reported that introduction of M476I into F32 parasites resulted in a modest gain of

157 resistance (mean survival of 1.7%) while this same mutation conferred RSA survival levels of ~10% in edited
158 Dd2 parasites (Straimer *et al*., 2015). These data suggest that while K13 mutations differ substantially in their
159 impact on ART susceptibility, there is an equally notable contribution of the parasite genetic background.
160
161 We next introduced M579I and C580Y into cloned Ugandan isolates UG659 and UG815. Editing of both
162 mutations into UG659 yielded moderate RSA survival rates (means of 6.3% and 4.7% for $UG659^{M579I}$ or
163 $UG659^{C580Y}$ respectively, vs. 1.0% for $UG659^{WT}$; **Figure 2C**). These values resembled our results with 3D7.
164 Strikingly, introducing K13 M579I or C580Y into UG815 yielded the highest rates of *in vitro* resistance, with
165 mean survival levels reaching ~12% in both $UG815^{M579I}$ and $UG815^{C580Y}$. These results were confirmed in a
166 second independent clone of $UG815^{M579I}$ (**Figure 2D**). M579I and C580Y also conferred equivalent levels of
167 resistance in edited Dd2 parasites (RSA survival rates of 4.0% and 4.7%, respectively; **Figure 2–source data**
168 **1**). These data show that mutant K13-mediated ART resistance in African parasites can be achieved, in some
169 but not all strains, at levels comparable to or above those seen in SE Asian parasites.
170
171 **K13 C580Y and M579I mutations, but not R561H, are associated with an *in vitro* fitness defect across**
172 **African parasites**
173 To examine the relation between resistance and fitness in African parasites harboring K13 mutations, we
174 developed an *in vitro* fitness assay that uses quantitative real-time PCR (qPCR) for allelic discrimination. Assays
175 were conducted by pairing K13 wild-type lines (i.e. 3D7, F32, UG659 and UG815) with their isogenic edited
176 R561H, M579I, or C580Y counterparts.
177
178 Assays were initiated with tightly synchronized trophozoites, mixed in 1:1 ratios of wild-type to mutant isogenic
179 parasites, and cultures were maintained over a period of 36 days (~18 generations of asexual blood stage
180 growth). Cultures were sampled every four days for genomic DNA (gDNA) preparation and qPCR analysis.
181 TaqMan probes specific to the *K13* wild-type or mutant (R561H, M579I or C580Y) alleles were used to quantify
182 the proportion of each allele.
183
184 Results showed that the K13 M579I and C580Y mutations each conferred a significant fitness defect across
185 most strains tested, with the proportions of K13 mutant lines declining over time. For both mutations, the largest

reductions were observed with edited 3D7 or UG815 parasites. In contrast, these mutations exerted a minimal impact on fitness in UG659. For R561H, we observed no impact on fitness in 3D7 parasites, although in F32 this mutation exerted a fitness defect similar to M579I and C580Y (**Figure 3A–D; Figure 3–source data 1**). From these data, we calculated the fitness cost, which represents the percent reduction in growth rate per 48 h generation of a test line compared to its wild-type isogenic comparator. These costs ranged from <1% to 12% per generation across mutations and lines, with the lowest costs observed in $3D7^{R561H}$ and $UG659^{C580Y}$, and the greatest cost observed with *K13*-edited UG815 lines (**Figure 3E**). Comparing data across these four African strains revealed that high RSA survival rates were generally accompanied by high fitness costs, and conversely that low fitness costs were associated with low survival rates. An exception was $3D7^{R561H}$ that showed moderate resistance with no apparent fitness cost (**Figure 3F**).

The K13 C580Y mutation has swept rapidly across Cambodia, displacing other K13 variants

We next examined the spatio-temporal distribution of *K13* alleles in Cambodia, the epicenter of ART resistance in SE Asia. In total, we analyzed the K13 propeller domain sequences from 3,327 parasite isolates collected from western, northern, eastern and southern Cambodian provinces (**Figure 4–figure supplement 1**). Samples were collected between 2001 and 2017, except for the southern region where sample collection was initiated in 2010. 1,412 samples (42%) were obtained and sequenced during the period 2015-2017 and have not previously been published. Earlier samples were reported in (Ariey *et al.*, 2014; Menard *et al.*, 2016). In sum, 19 nonsynonymous polymorphisms in K13 were identified across all regions and years. Of these, only three were present in >10 samples: Y493H (n=83), R539T (n=87) and C580Y (n=1,915). Each of these mutations was previously shown to confer ART resistance *in vitro* (Straimer *et al.*, 2015). Rarer mutations included A418V, I543T, P553L, R561H, P574L, and D584V (**Figure 4; Figure 4–source data 1**).

This analysis revealed a significant proportion of K13 wild-type parasites in the early 2000s, particularly in northern and eastern Cambodia, where 96% of isolates in 2001-2002 were wild type (**Figure 4**). In western Cambodia, where ART resistance first emerged (Dondorp *et al.*, 2009; Noedl *et al.*, 2009), the wild-type allele percentage in 2001-2002 had already fallen to 56%. This is striking given that delayed parasite clearance following ACT or artesunate treatment was first documented in 2008-2009 (Noedl *et al.*, 2008; Noedl *et al.*, 2009).

In all four regions, the frequency of the wild-type allele declined substantially over time and the diversity of mutant alleles contracted, with nearly all wild-type and non-K13 C580Y mutant parasites being replaced by parasites harboring the C580Y mutation (**Figure 4**). This effect was particularly pronounced in the west and the south, where the prevalence of C580Y in 2016-17 effectively attained 100%, increasing from 22% and 58% respectively in the initial sample sets (**Figure 4A, D**). In northern and eastern Cambodia, C580Y also outcompeted all other mutant alleles; however, 19-25% of parasites remained K13 wild type in 2016-17 (**Figure 4B, C**). These data show rapid dissemination of K13 C580Y across Cambodia.

SE Asian K13 mutations associated with delayed parasite clearance differ substantially in their ability to confer artemisinin resistance *in vitro*

Given that most K13 polymorphisms present in the field have yet to be characterized *in vitro*, we selected a set of mutations to test by gene editing, namely E252Q, F446I, P553L, R561H and P574L (highlighted in **Supplementary file 3**). F446I is the predominant mutation in Myanmar (Imwong *et al.*, 2020). P553L, R561H and P574L have each been shown to have multiple independent origins throughout SE Asia (Menard *et al.*, 2016), and were identified at low frequencies in our sequencing study in Cambodia (**Figure 4**). Lastly, the E252Q mutation was formerly prevalent on the Thai-Myanmar border, and, despite its occurrence upstream of the beta-propeller domain, has been associated with delayed parasite clearance *in vivo* (Anderson *et al.*, 2017; Cerqueira *et al.*, 2017; WWARN, 2019).

Zinc-finger nuclease- or CRISPR/Cas9-based gene-edited lines expressing K13 E252Q, F4461, P553L, R561H or P574L were generated in Dd2 or Cam3.II lines expressing wild-type K13 ($Dd2^{WT}$ or $Cam3.II^{WT}$) and recombinant parasites were cloned. Early ring-stage parasites were then assayed for their ART susceptibility using the RSA. For comparison, we included published Dd2 and Cam3.II lines expressing either K13 C580Y ($Dd2^{C580Y}$ and $Cam3.II^{C580Y}$) or R539T ($Dd2^{R539T}$ and the original parental line $Cam3.II^{R539T}$) (Straimer *et al.*, 2015), as well as control lines expressing only the guide-specific silent shield mutations ($Dd2^{ctrl}$ and $Cam3.II^{ctrl}$).

Both the P553L and R561H mutations yielded mean RSA survival rates comparable to C580Y (4.6% or 4.3% RSA survival for $Dd2^{P553L}$ or $Dd2^{R561H}$, respectively, vs 4.7% for $Dd2^{C580Y}$; **Figure 5A; Figure 5–source data 1**).

F446I and P574L showed only modest increases in survival relative to the wild-type parental line (2.0% and 2.1% for Dd2^{F446I} and Dd2^{P574L}, respectively, vs 0.6% for Dd2^{WT}). No change in RSA survival relative to Dd2^{WT} was observed for the Dd2^{E252Q} line. The resistant benchmark Dd2^{R539T} showed a mean RSA survival level of 20.0%, consistent with earlier reports of this mutation conferring high-grade ART resistance *in vitro* (Straimer *et al.*, 2015; Straimer *et al.*, 2017).

In contrast to Dd2, editing of the F446I, P553L and P574L mutations into Cambodian Cam3.II^{WT} parasites did not result in a statistically significant increase in survival relative to the K13 wild-type line, in part because the background survival rate of Cam3.II^{WT} was higher than for Dd2^{WT}. All survival values were <3%, contrasting with the Cam3.II^{R539T} parental strain that expresses the R539T mutation (~20% mean survival; **Figure 5B; Figure 5–source data 1**). The E252Q mutation did not result in elevated RSA survival in the Cam3.II background, a result also observed with Dd2. Nonetheless, ART resistance was apparent upon introducing the R561H mutation into Cam3.II^{WT} parasites, whose mean survival rates exceeded the Cam3.II^{C580Y} line (13.2% vs 10.0%, respectively). No elevated survival was seen in the Cam3.II^{ctrl} line expressing only the silent shield mutations used at the guide RNA cut site.

SE Asian K13 mutations do not impart a significant fitness impact on Dd2 parasites

Prior studies with isogenic gene-edited SE Asian lines have shown that certain K13 mutations can exert fitness costs, as demonstrated by reduced intra-erythrocytic asexual blood stage parasite growth (Straimer *et al.*, 2017; Nair *et al.*, 2018). To determine the fitness impact of the K13 mutations described above, we utilized an eGFP-based parasite competitive growth assay (Ross *et al.*, 2018). Dd2^{E252Q}, Dd2^{F446I}, Dd2^{P553L}, Dd2^{R561H} or Dd2^{P574L} were co-cultured with an isogenic K13 wild-type eGFP^{+} Dd2 reporter line at a starting ratio of 1:1. The proportion of eGFP^{+} parasites was then assessed every two days. As controls, we included Dd2^{WT}, Dd2^{bsm} and Dd2^{C580Y}. These data provided evidence of a minimal impact with the F446I, P553L and C580Y mutations, with E252Q, R561H and P574L having greater fitness costs when compared to Dd2^{WT} (**Figure 5C; Figure 5–figure supplement 1; Figure 5–source data 2**). Both C580Y and P553L displayed elevated RSA survival and minimal fitness cost in the Dd2 strain, providing optimal traits for dissemination (**Figure 5D**). We note that all fitness costs in Dd2 were considerably lower than those observed in our four African strains (**Figure 3**).

Strain-dependent genetic background differences significantly impact RSA survival rates in culture-adapted Thai isolates

Given the earlier abundance of the R561H and E252Q alleles in border regions of Thailand and Myanmar, we next tested the impact of introducing these mutations into five Thai K13 wild-type isolates (Thai1-5). For comparison, we also edited C580Y into several isolates. These studies revealed a major contribution of the parasite genetic background in dictating the level of mutant K13-mediated ART resistance, as exemplified by the C580Y lines whose mean survival rates ranged from 2.1% to 15.4%. Trends observed for individual mutations were maintained across strains, with the R561H mutation consistently yielding moderate to high *in vitro* resistance at or above the level of C580Y. Consistent with our Dd2 results, introducing E252Q did not result in significant increases in survival rates relative to isogenic K13 wild-type lines (**Figure 6A-E; Figure 6–source data 1**).

We also profiled two unedited culture-adapted Thai isolates (Thai6^{E252Q} and Thai7^{E252Q}) that express the K13 E252Q mutation upstream of the propeller domain. Notably, both lines exhibited mean RSA survival rates significantly above the 1% threshold for ART sensitivity (2.7% for Thai6^{E252Q} and 5.1% for Thai7^{E252Q}; **Figure 6F**). These data suggest that additional genetic factors present in these two Thai isolates are required for E252Q to manifest ART resistance.

Mutations in the *P. falciparum multidrug resistance protein 2* and *ferredoxin* genes do not modulate resistance to artemisinin or parasite fitness *in vitro*

In a prior genome-wide association study of SE Asian parasites, K13-mediated ART resistance was associated with D193Y and T484I mutations in the *ferredoxin* (*fd*) and *multidrug resistance protein 2* (*mdr2*) genes, respectively (Miotto *et al*., 2015). To directly test their role, we applied CRISPR/Cas9 editing (**Supplementary file 6**) to revert the fd D193Y and mdr2 T484I mutations to the wild-type sequences in the Cambodian strains RF7^{C580Y} and Cam3.II^{C580Y}, which both express K13 C580Y. Isogenic RF7^{C580Y} parasites expressing the mutant or wild-type fd residue at position 193 showed no change in RSA survival rates, either at 700 nM (averaging ~27%), or across a range of DHA concentrations down to 1.4 nM **(Figure 7A, C; Figure 7–figure supplement 1; Figure 7–source data 1**). Editing fd D193Y into the recombinant CamWT^{C580Y} line that expresses K13 C580Y (Straimer *et al*., 2015) also had no impact on RSA survival (with mean RSA survival rates of 11-13%).

Likewise, Cam3.II^{C580Y} parasites maintained the same rate *of in vitro* RSA survival (mean 19-22%) irrespective of their *mdr2* allele. Silent shield mutations had no impact for either *fd* or *mdr2*. eGFP-based fitness assays initiated at different starting ratios of eGFP and either *fd*-edited RF7^{C580Y} or *mdr2*-edited Cam3.II^{C580Y} lines revealed no change in the growth rates of the *fd* or *mdr2* mutants compared with their wild-type controls **(Figure 7B, D; Figure 7–figure supplement 1; Figure 7–source data 2 and 3**). These data suggest that the fd D193Y and mdr2 T484I mutations are markers of ART-resistant founder populations but themselves do not contribute directly to ART resistance or augment parasite fitness.

Discussion

Mutant K13-mediated ART resistance has substantially compromised the efficacy of antimalarial treatments across SE Asia (Hanboonkunupakarn and White, 2020), and the relatively high prevalence of the R561H variant that has recently been associated with delayed clearance in Rwanda highlights the risk of ART resistance emerging and spreading in sub-Saharan Africa (Uwimana *et al.*, 2020; Bergmann *et al.*, 2021; Uwimana *et al.*, 2021). Using gene editing and phenotypic analyses, we provide definitive evidence that the K13 R561H, M579I and C580Y mutations can confer *in vitro* ART resistance in several African strains. *In vitro* resistance, as defined using the RSA, was comparable between gene-edited K13 R561H 3D7 parasites (originating from or near Rwanda) and C580Y Dd2 and Cam3.II parasites (from SE Asia). Further investigations into edited African 3D7 parasites showed that these mutations also resulted in a ~30% decrease in K13 protein levels, consistent with earlier studies into the mechanistic basis of mutant K13-mediated ART resistance (Birnbaum *et al.*, 2017; Siddiqui *et al.*, 2017; Yang *et al.*, 2019; Gnadig *et al.*, 2020; Mok *et al.*, 2021). We also observed that K13 mutant African strains differed widely in their RSA survival rates. As an example, when introduced into the Tanzanian F32 strain, the C580Y mutation yielded a 0.3% RSA survival rate (not resistant), contrasting with 11.8% survival (highly resistant) in the Ugandan UG815 strain. These data suggest that F32 parasites lack additional genetic determinants that are required for mutant K13 to confer ART resistance. Collectively, our results provide evidence that certain African strains present no major biological obstacle to becoming ART resistant *in vitro* upon acquiring K13 mutations. Further gene editing experiments are merited to extend these studies to additional African strains, and to incorporate other variants such as C469Y and A675V that are increasing in prevalence in Uganda (Asua *et al.*, 2020).

Our mixed culture competition assays with African parasites revealed substantial fitness costs with the K13 C580Y mutation in three of the four strains tested (UG659 was the exception). The largest growth defect was observed with the edited UG815 C580Y line, which also yielded the highest level of ART resistance *in vitro*. These data suggest that K13 C580Y may not easily take hold in Africa where, unlike in SE Asia, infections are often highly polyclonal, generating intra-host competition that impacts a strain's ability to succeed at the population level. In addition, individuals in highly-endemic African settings generally have high levels of acquired immunity, potentially minimizing infection by relatively unfit parasites, and often have asymptomatic infections that go untreated, and are thus less subject to selective drug pressure, compared with individuals in SE Asia (Eastman and Fidock, 2009). This situation recalls the history of chloroquine use in Africa, where fitness costs caused by mutations in the primary resistance determinant PfCRT resulted in the rapid resurgence of wild-type parasites following the implementation of other first-line antimalarial therapies (Kublin *et al.*, 2003; Laufer *et al.*, 2006; Ord *et al.*, 2007; Frosch *et al.*, 2014).

An even greater fitness cost was observed with the M579I mutation, earlier detected in an infection acquired in Equatorial Guinea with evidence of *in vivo* ART resistance (Lu *et al.*, 2017) but which was notably absent in all 3,257 African samples reported herein. In contrast, we observed no evident fitness cost in 3D7 parasites expressing the R561H variant, which might help contribute to its increasing prevalence in Rwanda. While our Rwandan samples from 2012-2015 observed this mutation at 2% prevalence, samples collected by others in 2018 and 2019 identified this mutation at 12-13% prevalence (Bergmann *et al.*, 2021; Uwimana *et al.*, 2021). One of these reports included evidence associating R561H with delayed parasite clearance in patients treated with the ACT artemether-lumefantrine (Uwimana *et al.*, 2021). These recent data heighten the concern that mutant K13 might be taking hold in certain areas in in Africa where it can begin to compromise ACT efficacy.

In Cambodia, our spatio-temporal analysis of K13 sequence diversity highlights the initial emergence of C580Y in the western provinces, and its progressive replacement of other variants in the country. Interestingly, this mutation was already at high prevalence in western Cambodia several years before the first published reports of delayed parasite clearance in ART-treated patients (Noedl *et al.*, 2008; Dondorp *et al.*, 2009; Ariey *et al.*, 2014). The success of this mutation in Cambodia, and elsewhere in the eastern Greater Mekong subregion (Imwong *et*

359 *al.*, 2020), cannot be explained by resistance alone, as we previously reported that the less common R539T and
360 I543T variants conferred greater ART resistance *in vitro* (Straimer *et al.*, 2015). Similarly, we now report that the
361 R561H and P553L mutations yield equivalent degrees of ART resistance in Dd2 parasites when compared with
362 C580Y. In contrast, low-level resistance was observed with F446I, which has nonetheless spread across
363 Myanmar (Imwong *et al.*, 2020). In a separate recent gene editing study, F446I yielded no significant *in vitro*
364 resistance in 3D7 parasites and was fitness neutral (Siddiqui *et al.*, 2020), consistent with our findings for this
365 mutation in edited Dd2 parasites.
366
367 Our studies into the impact of K13 mutations on *in vitro* growth in Asian Dd2 parasites provide evidence that that
368 the C580Y mutation generally exerts less of a fitness cost relative to other K13 variants, as measured in *K13*-
369 edited parasites co-cultured with an eGFP reporter line. A notable exception was P553L, which compared with
370 C580Y was similarly fitness neutral and showed similar RSA values. P553L has nonetheless proven far less
371 successful in its regional dissemination compared with C580Y (Menard *et al.*, 2016). These data suggest that
372 additional factors have contributed to the success of C580Y in sweeping across SE Asia. These might include
373 specific genetic backgrounds that have favored the dissemination of C580Y parasites, possibly resulting in
374 enhanced transmission potential (Witmer *et al.*, 2020), or ACT use that favored the selection of partner drug
375 resistance in these parasite backgrounds (van der Pluijm *et al.*, 2019). In terms of growth rates in our isogenic
376 Dd2 lines, the most detrimental impacts were observed with E252Q and R561H, which earlier predominated
377 near the Thailand-Myanmar border region, but were later overtaken by C580Y (Phyo *et al.*, 2016). In our study,
378 C580Y produced an optimal combination of no measurable fitness cost and relatively high RSA survival rates in
379 Dd2 parasites. In a prior independent study however, R561H showed slightly improved fitness relative to C580Y
380 in paired isogenic parasites from Thailand (generated in the NHP4302 strain), providing further evidence that
381 both fitness and resistance are strain-dependent (Nair *et al.*, 2018).
382
383 Further research is also required to define secondary genetic determinants that could augment mutant K13-
384 mediated ART resistance, and to explore other potential mediators of resistance. Proposed candidates have
385 included *fd*, *mdr2*, *ap-2μ*, *ubp1* and *pfcoronin*, which have earlier been associated with *P. falciparum* ART
386 susceptibility (Demas *et al.*, 2018; Henrici *et al.*, 2019; Sutherland *et al.*, 2020). Our data argue against a direct
387 role for mutations in *fd* and *mdr2* in the strains tested herein. We also observed no evident association between

388 the genotypes of *pfcrt*, *pfmdr1*, *arps10*, *ap-2μ* or *ubp1* and the degree to which mutant K13 conferred ART
389 resistance *in vitro* in our set of African or Asian strains (**Supplementary file 4**). Mutations associated with
390 enhanced DNA repair mechanisms have also been observed in ART-resistant SE Asian parasites, supporting
391 the idea that mutant K13 parasites may have an improved ability to repair ART-mediated DNA damage (Xiong
392 *et al*., 2020). Further studies are merited to investigate whether these DNA repair mutations may provide a
393 favorable background for the development of ART resistance.
394
395 At the population level, we note that *P. falciparum* genomic structures in Africa tend to be far more diverse than
396 in the epicenter of resistance in Cambodia, where parasite strains are highly sub-structured into a few lineages
397 that can readily maintain complex genetic traits (Amato *et al*., 2018). A requirement to transmit mutant K13 and
398 additional determinants of resistance in African malaria-endemic settings, where genetic outcrossing is the
399 norm, would predict that ART resistance will spread more gradually in this continent than in SE Asia. It is
400 nonetheless possible that secondary determinants will allow some African strains to offset fitness costs
401 associated with mutant K13, or otherwise augment K13-mediated ART resistance. Identifying such determinants
402 could be possible using genome-wide association studies or genetic crosses between ART-resistant and
403 sensitive African parasites in the human liver-chimeric mouse model of *P. falciparum* infection (Vaughan *et al*.,
404 2015; Amambua-Ngwa *et al*., 2019). Reduced transmission rates in areas of Africa where malaria is declining,
405 leading to lower levels of immunity, may also benefit the emergence and dissemination of mutant K13 (Conrad
406 and Rosenthal, 2019).
407
408 Another impediment to the dissemination of ART resistance in Africa is the continued potent activity of
409 lumefantrine, the partner drug in the first line treatment artemether-lumefantrine (Conrad and Rosenthal, 2019).
410 This situation contrasts with SE Asia where ART-resistant parasites have also developed high-level resistance
411 to the partner drug PPQ, with widespread treatment failures enabling the dissemination of multidrug-resistant
412 strains (Conrad and Rosenthal, 2019; van der Pluijm *et al*., 2019). While the genotyping data presented herein
413 and other recent molecular surveillance studies reveal low prevalence of mutant K13 in Africa (Kayiba *et al*.,
414 2020; Schmedes *et al*., 2021), the emergence and spread of the R561H variant in Rwanda is cause for
415 significant concern. These data call for continuous continent-wide monitoring of the emergence and spread of

mutant K13 in Africa, and for studies into whether its emergence in Rwanda is a harbinger of subsequent partner drug resistance and ACT treatment failure.

Materials and Methods

Key Resources Table

Reagent type (species) or resource	Designation	Source or reference	Identifiers	Additional information
Gene (*Plasmodium falciparum* 3D7 strain)	*Kelch13* (*K13*)	PlasmoDB	PF3D7_1343700	
Gene (*Plasmodium falciparum* 3D7 strain)	*Ferredoxin* (*fd*)	PlasmoDB	PF3D7_1318100	
Gene (*Plasmodium falciparum* 3D7 strain)	*Multidrug resistance protein 2* (*mdr2*)	PlasmoDB	PF3D7_1447900	
Strain, strain background (*Plasmodium falciparum*)	3D7 clone A10 ($3D7^{WT}$)	D. Goldberg, Washington University School of Medicine, St. Louis, MO, USA		see **Table 1** and **Supplementary file 4** for additional details on all *P. falciparum* strains employed herein
Strain, strain background (*Plasmodium falciparum*)	F32-TEM ($F32^{WT}$)	F. Benoit-Vical, Université de Toulouse, Toulouse, France (Ariey *et al.*, 2014)		
Strain, strain background (*Plasmodium falciparum*)	UG659 ($UG659^{WT}$)	P. Rosenthal, University of California, San Francisco, CA, USA		
Strain, strain background (*Plasmodium falciparum*)	UG815 ($UG815^{WT}$)	P. Rosenthal, University of California, San Francisco, CA, USA		
Strain, strain background (*Plasmodium falciparum*)	Dd2 ($Dd2^{WT}$)	The Malaria Research and Reference Reagent Resource Center (MR4), BEI Resources	MRA-156	
Strain, strain background (*Plasmodium falciparum*)	Cam3.II ($Cam3.II^{R539T}$)	R. Fairhurst, NIAID, NIH, Bethesda, MD, USA (Straimer *et al.*, 2015)	PH0306-C	

Strain, strain background (*Plasmodium falciparum*)	CamWT	R. Fairhurst, NIAID, NIH, Bethesda, MD, USA (Straimer *et al*., 2015)	PH0164-C	
Strain, strain background (*Plasmodium falciparum*)	RF7 ($RF7^{C580Y}$)	R. Fairhurst, NIAID, NIH, Bethesda, MD, USA (Ross *et al*., 2018)	PH1008-C	
Strain, strain background (*Plasmodium falciparum*)	$Thai1^{WT}$	T. Anderson, Texas Biomedical Research Institute, San Antonio, TX, USA	TA32A2A4	
Strain, strain background (*Plasmodium falciparum*)	$Thai2^{WT}$	T. Anderson, Texas Biomedical Research Institute, San Antonio, TX, USA	TA50A2B2	
Strain, strain background (*Plasmodium falciparum*)	$Thai3^{WT}$	T. Anderson, Texas Biomedical Research Institute, San Antonio, TX, USA	TA85R1	
Strain, strain background (*Plasmodium falciparum*)	$Thai4^{WT}$	T. Anderson, Texas Biomedical Research Institute, San Antonio, TX, USA	TA86A3	
Strain, strain background (*Plasmodium falciparum*)	$Thai5^{WT}$	T. Anderson, Texas Biomedical Research Institute, San Antonio, TX, USA	NHP-01334-6B	
Strain, strain background (*Plasmodium falciparum*)	$Thai6^{E252Q}$	T. Anderson, Texas Biomedical Research Institute, San Antonio, TX, USA	NHP4076	
Strain, strain background (*Plasmodium falciparum*)	$Thai7^{E252Q}$	T. Anderson, Texas Biomedical Research Institute, San Antonio, TX, USA	NHP4673	
Strain, strain background (*Escherichia coli*)	HST08	Takara	Cat. #636766	Stellar™ Competent Cells

Genetic reagent (*Plasmodium falciparum*)	Transgenic parasite lines	This study and (Straimer *et al*., 2015)	See **Supplementary file 5**	Available from D. Fidock upon request
Commercial assay or kit	In-Fusion® HD Cloning Plus kit	Takara	Cat. #638909	
Commercial assay or kit	QuantiFast Multiplex PCR Kit	Qiagen	Cat. #204654	
Sequence-based reagents	Oligonucleotides	This study	See **Supplementary file 7**	
Recombinant DNA reagents	Plasmids	This study	See **Supplementary file 8**	Available from D. Fidock upon request
Sequence-based reagents	qPCR primers and probes	This study	See **Supplementary file 9**	
Antibody	Anti-K13 (*P. falciparum*) (Mouse monoclonal)	I. Trakht, Columbia University Medical Center, New York, NY, USA (Gnadig *et al*., 2020)		Antibody clone E9 WB (1:1000)
Antibody	Anti-ERD2 (*P. falciparum*) (Rabbit polyclonal)	MR4, BEI Resources	MRA-1	WB (1:1000)
Antibody	StarBright Blue 700 goat anti-mouse	Bio-Rad	12004158	WB (1:200)
Antibody	StarBright Blue 520 goat anti-rabbit	Bio-Rad	12005869	WB (1:1000)
Other	4–20% Criterion™ TGX™ Precast Protein Gel	Bio-Rad	5671093	Used with recommended buffers, also purchased from Bio-Rad
Chemical compound, drug	Carbenicillin disodium salt	Sigma	C1389	
Chemical compound, drug	WR99210	Jacobus Pharmaceuticals		
Chemical compound, drug	Dihydroartemisinin (DHA)	Sigma	D7439	

Software, algorithm	GraphPad Prism Version 9	GraphPad Software, San Diego, CA, USA		graphpad.com
Software, algorithm	ImageJ software	NIH, Bethesda, MD, USA		imagej.nih.gov

Sample collection and *K13* genotyping

Samples were obtained as blood-spot filter papers from patients seeking treatment at sites involved in national surveys of antimalarial drug resistance, or patients enrolled in therapeutic efficacy studies, or asymptomatic participants enrolled in surveillance programs. Collection details from African and Cambodian samples are provided in **Figure 1–source data 1** and **Figure 4–source data 1**, respectively. Samples were processed at the Pasteur Institute in Paris or the Pasteur Institute in Cambodia, as detailed in **Supplementary file 1**. These investigators vouch for the accuracy and completeness of the molecular data. DNA was extracted from dried blood spots using QIAmp Mini kits, as described (Menard *et al.*, 2016). A nested PCR was performed on each sample to amplify the *K13*-propeller domain, corresponding to codons 440-680. PCR products were sequenced using internal primers and electropherograms analyzed on both strands, using the Pf3D7_1343700 3D7 sequence as the wild-type reference. Quality controls included adding six blinded quality-control samples to each 96-well sequencing plate prepared from samples from each in-country partner and independently retesting randomly selected blood samples. Isolates with mixed alleles were considered to be mutated for the purposes of estimating the mutation frequencies.

P. falciparum parasite *in vitro* culture

Plasmodium falciparum asexual blood-stage parasites were cultured in human erythrocytes at 3% hematocrit in RPMI-1640 medium supplemented with 2 mM L-glutamine, 50 mg/L hypoxanthine, 25 mM HEPES, 0.21% NaHCO3, 10 mg/L gentamycin and 0.5% w/v Albumax II (Invitrogen). Parasites were maintained at 37ºC in 5% O_2, 5% CO_2, and 90% N_2. The geographic origin and year of culture adaptation for lines employed herein are described in **Supplementary file 4**. Parasite lines were authenticated by genotyping resistance genes and were screened by PCR for Mycoplasma every 3-6 months.

Whole-genome sequencing of parental lines

To define the genome sequences of our *P. falciparum* lines used for transfection, we lysed parasites in 0.05% saponin, washed them with 1×PBS, and purified genomic DNA (gDNA) using the QIAamp DNA Blood Midi Kit (Qiagen). DNA concentrations were quantified by NanoDrop (Thermo Scientific) and Qubit (Invitrogen) prior to sequencing. 200 ng of gDNA was used to prepare sequencing libraries using the Illumina Nextera DNA Flex library prep kit with dual indices. Samples were multiplexed and sequenced on an Illumina MiSeq to obtain 300 bp paired-end reads at an average of 50× depth of coverage. Sequence reads were aligned to the *P. falciparum* 3D7 reference genome (PlasmoDB version 36) using Burrow-Wheeler Alignment. PCR duplicates and unmapped reads were filtered out using Samtools and Picard. Reads were realigned around indels using GATK RealignerTargetCreator and base quality scores were recalibrated using GATK BaseRecalibrator. GATK HaplotypeCaller (version 3.8) was used to identify all single nucleotide polymorphisms (SNPs). These SNPs were filtered based on quality scores (variant quality as function of depth QD > 1.5, mapping quality > 40, min base quality score > 18) and read depth (> 5) to obtain high-quality SNPs, which were annotated using snpEFF. Integrated Genome Viewer was used to visually verify the presence of SNPs. BIC-Seq was used to check for copy number variations using the Bayesian statistical model (Xi *et al*., 2011). Copy number variations in highly polymorphic surface antigens and multi-gene families were removed as these are prone to stochastic changes during *in vitro* culture.

Whole-genome sequencing data were used to determine the genotypes of the antimalarial drug resistance loci *pfcrt*, *mdr1*, *dhfr* and *dhps* (Haldar *et al*., 2018). We also genotyped *fd*, *arps10*, *mdr2*, *ubp1,* and *ap-2μ*, which were previously associated with ART resistance (Henriques *et al*., 2014; Miotto *et al*., 2015; Cerqueira *et al*., 2017; Adams *et al*., 2018). These results are described in **Supplementary file 4.**

Cloning of *K13, fd* and *mdr2* plasmids

Zinc-finger nuclease-meditated editing of select mutations in the *K13* locus was performed as previously described (Straimer *et al*., 2015). CRISPR/Cas9 editing of *K13* mutations was achieved using the pDC2-cam-coSpCas9-U6-gRNA-h*dhfr* all-in-one plasmid that contains a *P. falciparum* codon-optimized Cas9 sequence, a human dihydrofolate reductase (h*dhfr*) gene expression cassette (conferring resistance to WR99210) and restriction enzyme insertion sites for the guide RNA (gRNA) and donor template (White *et al*., 2019). A K13

propeller domain-specific gRNA was introduced into this vector at the BbsI restriction sites using the primer pair p1+p2 (**Supplementary file 7**) using T4 DNA ligase (New England BioLabs). Oligos were phosphorylated and annealed prior to cloning. A donor template consisting of a 1.5 kb region of the *K13* coding region including the entire propeller domain was amplified using the primer pair p3+p4 and cloned into the pGEM T-easy vector system (Promega). This donor sequence was subjected to site-directed mutagenesis in the pGEM vector to introduce silent shield mutations at the Cas9 cleavage site using the primer pair p5+p6, and to introduce allele-specific mutations using primer pairs (p7 to p20). *K13* donor sequences were amplified from the pGEM vector using the primer pair p21+p22 and sub-cloned into the pDC2-cam-coSpCas9-U6-gRNA-h*dhfr* plasmid at the EcoRI and AatII restriction sites by In-Fusion Cloning (Takara). Final plasmids (see **Supplementary file 8**) were sequenced using primers p23 to p25. A schematic showing the method of *K13* plasmid construction can be found in **Supplementary file 2**. Both our customized zinc-finger nuclease and CRISPR/Cas9 approaches generated the desired amino acid substitutions without the genomic integration of any plasmid sequences or any additional amino acid changes in the K13 locus, and thus provide fully comparable data.

CRISPR/Cas9 editing of *fd* and *mdr2* was performed using a separate all-in-one plasmid, pDC2-cam-Cas9-U6-gRNA-h*dhfr*, generated prior to the development of the codon-optimized version used above for *K13* (Lim *et al*., 2016). Cloning was performed as for *K13*, except for gRNA cloning that was performed using In-Fusion cloning (Takara) rather than T4 ligase. Cloning of gRNAs was performed using primer pair p29+p30 for *fd* and p42+p43 for *mdr2*. Donor templates were amplified and cloned into the final vector using the primer pairs p31+p32 for *fd* and p44+p45 for *mdr2*. Site-directed mutagenesis was performed using the allele-specific primer pairs p33+p34 or p35+p36 for *fd*, and p46+p47 or p48+p49 for *mdr2*. All final plasmids (for both *fd* and *mdr2*, see **Supplementary file 8**) were sequenced using the primer pair p37+p38 (**Supplementary file 7**). Schematic representations of final plasmids are shown in **Supplementary file 6**.

Generation of *K13*, *fd* and *mdr2* gene-edited parasite lines

Gene-edited lines were generated by electroporating ring-stage parasites at 5-10% parasitemia with 50 µg of purified circular plasmid DNA resuspended in Cytomix. Transfected parasites were selected by culturing in the presence of WR99210 (Jacobus Pharmaceuticals) for six days post electroporation. Parental lines harboring 2-3 mutations in the *P. falciparum* dihydrofolate reductase (*dhfr*) gene were exposed to 2.5 nM WR99210, while

parasites harboring four *dhfr* mutations were selected under 10 nM WR99210 (see **Supplementary file 4** for *dhfr* genotypes of transfected lines). Parasite cultures were monitored for recrudescence by microscopy for up six weeks post electroporation. To test for successful editing, the *K13* locus was amplified directly from parasitized whole blood using the primer pair p26+p27 (**Supplementary file 7**) and the MyTaq™ Blood-PCR Kit (Bioline). Primer pairs p39+p40 and p50+p51 were used to amplify *fd* and *mdr2*, respectively. PCR products were submitted for Sanger sequencing using the PCR primers as well as primer p28 in the case of *K13*, p41 (*fd*) or p52 (*mdr2*). Bulk-transfected cultures showing evidence of editing by Sanger sequencing were cloned by limiting dilution. All gene-edited transgenic lines generated herein are described in **Supplementary file 5**.

Parasite synchronization, ring-stage survival assays (RSAs) and flow cytometry

Synchronized parasite cultures were obtained by exposing predominantly ring-stage cultures to 5% D-Sorbitol (Sigma) for 15 min at 37°C to remove mature parasites. After 36 h of subsequent culture, multinucleated schizonts were purified over a density gradient consisting of 75% Percoll (Sigma). Purified schizonts were incubated with fresh RBCs for 3h, and early rings (0-3 hours post invasion; hpi) were treated with 5% D-Sorbitol to remove remaining schizonts.

In vitro RSAs were conducted as previously described, with minor adaptations (Straimer *et al.*, 2015). Briefly, tightly synchronized 0-3 hpi rings were exposed to a pharmacologically-relevant dose of 700 nM DHA or 0.1% dimethyl sulfoxide (DMSO; vehicle control) for 6 h at 1% parasitemia and 2% hematocrit, washed three times with RPMI medium to remove drug, transferred to fresh 96-well plates, and cultured for an additional 66 h in drug-free medium. Removal of media and resuspension of parasite cultures was performed on a Freedom Evo 100 liquid-handling instrument (Tecan). Parasitemias were measured at 72 h by flow cytometry (see below) with at least 50,000 events captured per sample. Parasite survival was expressed as the percentage value of the parasitemia in DHA-treated samples divided by the parasitemia in DMSO-treated samples processed in parallel. We considered any RSA mean survival rates <2% to be ART sensitive.

Flow cytometry was performed on an BD Accuri^{TM} C6 Plus cytometer with a HyperCyt plate sampling attachment (IntelliCyt), or on an iQue3® Screener Plus cytometer (Sartorius). Cells were stained with 1×SYBR Green (ThermoFisher) and 100 nM MitoTracker DeepRed (ThermoFisher) for 30 min and diluted in 1×PBS prior

to sampling. Percent parasitemia was determined as the percentage of MitoTracker$^-$positive and SYBR Green-positive cells. For RSAs, >50,000 events were captured per well.

Western blot analysis of K13 expression levels in edited lines

Western blots were performed with lysates from tightly synchronized rings harvested 0-6 h post invasion. Parasite cultures were washed twice in ice-cold 1× phosphate-buffered saline (PBS), and parasites isolated by treatment with 0.05% saponin in PBS. Released parasites were lysed in 4% SDS, 0.5% Triton X-100 and 0.5% PBS supplemented 1× protease inhibitors (Halt Protease Inhibitors Cocktail, ThermoFisher). Samples were centrifuged at 14,000 rpm for 10 min to pellet cellular debris. Supernatants were collected and protein concentrations were determined using the DC protein assay kit (Bio-Rad). Laemmli Sample Buffer (Bio-Rad) was added to lysates and samples were denatured at 90°C for 10 min. Proteins were electrophoresed on precast 4-20% Tris-Glycine gels (Bio-Rad) and transferred onto nitrocellulose membranes. Western blots were probed with a 1:1000 dilution of primary antibodies to K13 (Gnadig *et al*., 2020) or the loading control ERD2 (BEI Resources), followed by a 1:200 dilution of fluorescent StarBright secondary antibodies (Bio-Rad). Western blots were imaged on a ChemiDoc system (Bio-Rad) and band intensities quantified using ImageJ.

TaqMan allelic discrimination real-time (quantitative) PCR-based fitness assays

Fitness assays with African *K13*-edited parasite lines were performed by co-culturing isogenic wild-type unedited and mutant edited parasites in 1:1 ratios. Assays were initiated with tightly synchronized trophozoites. Final culture volumes were 3 mL. Cultures were maintained in 12-well plates and monitored every four days over a period of 36 days (18 generations) by harvesting at each time point a fraction of each co-culture for saponin lysis. gDNA was then extracted using the QIAamp DNA Blood Mini Kit (Qiagen). The percentage of the wild-type or mutant allele in each sample was determined in TaqMan allelic discrimination real-time PCR assays. TaqMan primers (forward and reverse) and TaqMan fluorescence-labeled minor groove binder probes (FAM or HEX, Eurofins) are described in **Supplementary file 9**. Probes were designed to specifically detect the K13 R561H, M579I or C580Y propeller mutations. The efficiency and sensitivity of the TaqMan primers was assessed using standard curves comprising 10-fold serially diluted templates ranging from 10 ng to 0.001 ng. Robustness was demonstrated by high efficiency (88-95%) and R^2 values (0.98-1.00). The quantitative accuracy in genotype calling was assessed by performing multiplex qPCR assays using mixtures of wild-type and mutant

plasmids in fixed ratios (0:100, 20:80, 40:60, 50:50, 60:40, 80:20, 100:0). Triplicate data points clustered tightly, indicating high reproducibility in the data across the fitted curve (R^2 = 0.89 to 0.91).

Purified gDNA from fitness co-cultures was subsequently amplified and labeled using the primers and probes described in **Supplementary file 9**. qPCR reactions for each sample were run in triplicate. 20 µL reactions consisted of 1×QuantiFAST reaction mix containing ROX reference dye (Qiagen), 0.66 µM of forward and reverse primers, 0.16 µM FAM-MGB and HEX-MGB TaqMan probes, and 10 ng genomic DNA. Amplification and detection of fluorescence were carried out on a QuantStudio 3 qPCR machine (Applied Biosystems) using the genotyping assay mode. Cycling conditions were as follows: 30s at 60°C; 5 min at 95°C; and 40 cycles of 30s at 95°C and 1 min at 60°C for primer annealing and extension. Every assay was run with positive controls (wild-type or mutant plasmids at different fixed ratios). No-template negative controls (water) in triplicates were processed in parallel. Rn, the fluorescence of the FAM or HEX probe, was normalized to the fluorescence signal of the ROX reporter dye. Background-normalized fluorescence (Rn minus baseline, or ΔRn) was calculated as a function of cycle number.

To determine the wild-type or mutant allele frequency in each sample, we first confirmed the presence of the allele by only retaining values where the threshold cycle (C_t) of the sample was less than the no-template control by at least three cycles. Next, we subtracted the ΔRn of the samples from the background ΔRn of the no-template negative control. We subsequently normalized the fluorescence to 100% using the positive control plasmids to obtain the percentage of the wild-type and mutant alleles for each sample. The final percentage of the mutant allele was defined as the average of these two values: the normalized percentage of the mutant allele, and 100% minus the normalized percentage of the wild-type allele.

eGFP-based fitness assays

Fitness assays with Dd2, RF7^{C580Y} and Cam3.II parasite lines were performed using mixed culture competition assays with an eGFP-positive (eGFP^{+}) Dd2 reporter line (Ross *et al*., 2018). This reporter line uses a *calmodulin* promoter sequence to express high levels of GFP and includes human *dhfr* and *blasticidin S-deaminase* expression cassettes. This line was earlier reported to have a reduced rate of growth relative to parental non-recombinant Dd2, presumably at least in part because of its high levels of GFP expression (Ross *et al*., 2018;

589 Dhingra *et al.*, 2019). With our Dd2 parasites, *K13*-edited lines were co-cultured in 1:1 ratios with the reporter
590 line. This ratio was adjusted to 10:1 or 100:1 for *fd*-edited RF7^{C580Y} and *mdr2*-edited Cam3.II parasites relative to
591 the eGFP line, given the slower rate of growth with RF7^{C580Y} and Cam3.II. Fitness assays were initiated with
592 tightly synchronized trophozoites in 96-well plates, with 200 µL culture volumes. Percentages of eGFP^{+}
593 parasites were monitored by flow cytometry every two days over a period of 20 days (10 generations). Flow
594 cytometry was performed as written above, except that only 100 nM MitoTracker DeepRed staining was used to
595 detect total parasitemias, since SYBR Green and eGFP fluoresce in the same channel.
596
597 **Fitness Costs**
598 The fitness cost associated with a line expressing a given K13 mutation was calculated was calculated relative
599 to its isogenic wild-type counterpart using the following equation:

$$P' = P((1 - x)^n)$$

600 where P' is equal to the parasitemia at the assay endpoint, P is equal to the parasitemia on day 0, n is equal to
601 the number of generations from the assay start to finish, and x is equal to the fitness cost. This equation
602 assumes 100% growth for the wild-type comparator line. For qPCR and GFP-based fitness assays, days 36 and
603 20 were set as the assay endpoints, resulting in the number of parasite generations (n) being set to 18 and 10,
604 respectively.
605

606 ## Ethics statement

607 Health care facilities were in charge of collecting anonymized *P. falciparum* positive cases. Identification of
608 individuals cannot be established. The studies were approved by ethics committees listed in **Supplementary**
609 **file 1**. We note that the sponsors had no role in the study design or in the collection or analysis of the data.
610 There was no confidentiality agreement between the sponsors and the investigators.
611

612 ## Acknowledgments

613 We thank Dr. Pascal Ringwald (World Health Organization) for his support and feedback. DAF gratefully
614 acknowledges the US National Institutes of Health (R01 AI109023), the Department of Defense
615 (W81XWH1910086) and the Bill & Melinda Gates Foundation (OPP1201387) for their financial support. BHS

was funded in part by T32 AI106711 (PD: D. Fidock). SM is a recipient of a Human Frontiers of Science Program Long-Term Fellowship. CHC was supported in part by the NIH (R01 AI121558; PI: Jonathan Juliano). FN is supported by the Wellcome Trust of Great Britain (Grant ID: 106698). TJCA acknowledges funding support from the NIH (R37 AI048071). DAF and DM gratefully acknowledge the World Health Organization for their funding. We thank the following individuals for their kind help with the *K13*-genotyped samples – Chad: Ali S. Djiddi, Mahamat S. I. Diar, Kodbessé Boulotigam, Mbanga Djimadoum, Hamit M. Alio, Mahamat M. H. Taisso, Issa A. Haggar; Burkina Faso: TES 2017-2018 team and the US President's Malaria Initiative through the Improving Malaria Care Project as the funding agency for the study in Burkina Faso, Chris-Boris G. Panté-Wockama; Burundi: Dismas Baza; Tanzania: Mwaka Kakolwa, Celine Mandara, Tanzania TES coordination team for the Ministry of Health; Sierra Leone: Anitta R. Y. Kamara, Foday Sahr, Mohamed Samai; The Gambia: Balla Kandeh, Joseph Okebe, Serign J. Ceesay, Baboucarr Babou, Emily Jagne, Alsan Jobe; Congo: Brice S. Pembet, Jean M. Youndouka; Somalia: Jamal Ghilan Hefzullah Amran, Abdillahi Mohamed Hassan, Abdikarim Hussein Hassan and Ali Abdulrahman; Rwanda: extended TES team for the Malaria and Other Parasitic Diseases Division, Rwanda Biomedical Centre.

Competing interests

MW is a former staff member of the World Health Organization. MW alone is responsible for the views expressed in this publication, which do not necessarily represent the decisions, policies or views of the World Health Organization. The other authors declare that no competing interests exist.

References

Adams T, Ennuson NAA, Quashie NB, Futagbi G, Matrevi S, Hagan OCK, Abuaku B, Koram KA, Duah NO. 2018. Prevalence of *Plasmodium falciparum* delayed clearance associated polymorphisms in adaptor protein complex 2 mu subunit (*pfap2mu*) and ubiquitin specific protease 1 (*pfubp1*) genes in Ghanaian isolates. *Parasit Vectors* **11**:175. DOI: https://doi.org/10.1186/s13071-018-2762-3. PMID: 29530100

Amambua-Ngwa A, Amenga-Etego L, Kamau E, Amato R, Ghansah A, Golassa L, Randrianarivelojosia M, Ishengoma D, Apinjoh T, Maiga-Ascofare O, Andagalu B, Yavo W, Bouyou-Akotet M, Kolapo O, Mane K, Worwui A, Jeffries D, Simpson V, D'Alessandro U, Kwiatkowski D, Djimde AA. 2019. Major subpopulations of *Plasmodium falciparum* in sub-Saharan Africa. *Science* **365**:813-816. DOI: https://doi.org/10.1126/science.aav5427. PMID: 31439796

Amato R, Pearson RD, Almagro-Garcia J, Amaratunga C, Lim P, Suon S, Sreng S, Drury E, Stalker J, Miotto O, Fairhurst RM, Kwiatkowski DP. 2018. Origins of the current outbreak of multidrug-resistant malaria in southeast Asia: a retrospective genetic study. *Lancet Infect Dis* **18**:337-345. DOI: https://doi.org/10.1016/S1473-3099(18)30068-9. PMID: 29398391

Anderson TJ, Nair S, McDew-White M, Cheeseman IH, Nkhoma S, Bilgic F, McGready R, Ashley E, Pyae Phyo A, White NJ, Nosten F. 2017. Population parameters underlying an ongoing soft sweep in Southeast Asian malaria parasites. *Mol Biol Evol* **34**:131-144. DOI: https://doi.org/10.1093/molbev/msw228. PMID: 28025270

Ariey F, Witkowski B, Amaratunga C, Beghain J, Langlois AC, Khim N, Kim S, Duru V, Bouchier C, Ma L, Lim P, Leang R, Duong S, Sreng S, Suon S, Chuor CM, Bout DM, Menard S, Rogers WO, Genton B, Fandeur T, Miotto O, Ringwald P, Le Bras J, Berry A, Barale JC, Fairhurst RM, Benoit-Vical F, Mercereau-Puijalon O, Menard D. 2014. A molecular marker of artemisinin-resistant *Plasmodium falciparum* malaria. *Nature* **505**:50-55. DOI: https://doi.org/10.1038/nature12876. PMID: 24352242

Ashley EA, Dhorda M, Fairhurst RM, Amaratunga C, Lim P, Suon S, Sreng S, Anderson JM, Mao S, Sam B, Sopha C, Chuor CM, Nguon C, Sovannaroth S, Pukrittayakamee S, Jittamala P, Chotivanich K, Chutasmit K, Suchatsoonthorn C, Runcharoen R, Hien TT, Thuy-Nhien NT, Thanh NV, Phu NH, Htut Y, Han KT, Aye KH, Mokuolu OA, Olaosebikan RR, Folaranmi OO, Mayxay M, Khanthavong M, Hongvanthong B, Newton PN, Onyamboko MA, Fanello CI, Tshefu AK, Mishra N, Valecha N, Phyo AP, Nosten F, Yi P, Tripura R, Borrmann S, Bashraheil M, Peshu J, Faiz MA, Ghose A, Hossain MA, Samad R, Rahman MR, Hasan MM, Islam A, Miotto O, Amato R, MacInnis B, Stalker J, Kwiatkowski DP, Bozdech Z, Jeeyapant A, Cheah PY, Sakulthaew T, Chalk J, Intharabut B, Silamut K, Lee SJ, Vihokhern B, Kunasol C, Imwong M, Tarning J, Taylor WJ, Yeung S, Woodrow CJ, Flegg JA, Das D, Smith J, Venkatesan M, Plowe CV, Stepniewska K, Guerin PJ, Dondorp AM, Day NP, White NJ, Tracking Resistance to Artemisinin Consortium. 2014. Spread of artemisinin resistance in P*lasmodium falciparum* malaria. *N Engl J Med* **371**:411-423. DOI: https://doi.org/10.1056/NEJMoa1314981. PMID: 25075834

Asua V, Conrad MD, Aydemir O, Duvalsaint M, Legac J, Duarte E, Tumwebaze P, Chin DM, Cooper RA, Yeka A, Kamya MR, Dorsey G, Nsobya SL, Bailey J, Rosenthal PJ. 2020. Changing prevalence of potential mediators of aminoquinoline, antifolate, and artemisinin resistance across Uganda. *J Infect Dis* **223**:985-994. DOI: https://doi.org/10.1093/infdis/jiaa687. PMID: 33146722

Bergmann C, van Loon W, Habarugira F, Tacoli C, Jager JC, Savelsberg D, Nshimiyimana F, Rwamugema E, Mbarushimana D, Ndoli J, Sendegeya A, Bayingana C, Mockenhaupt FP. 2021. Increase in Kelch 13 polymorphisms in *Plasmodium falciparum*, Southern Rwanda. *Emerg Infect Dis* **27**:294-296. DOI: https://doi.org/10.3201/eid2701.203527. PMID: 33350925

Birnbaum J, Flemming S, Reichard N, Soares AB, Mesen-Ramirez P, Jonscher E, Bergmann B, Spielmann T. 2017. A genetic system to study *Plasmodium falciparum* protein function. *Nat Methods* **14**:450-456. DOI: https://doi.org/10.1038/nmeth.4223. PMID: 28288121

Birnbaum J, Scharf S, Schmidt S, Jonscher E, Hoeijmakers WAM, Flemming S, Toenhake CG, Schmitt M, Sabitzki R, Bergmann B, Frohlke U, Mesen-Ramirez P, Blancke Soares A, Herrmann H, Bartfai R, Spielmann T. 2020. A Kelch13-defined endocytosis pathway mediates artemisinin resistance in malaria parasites. *Science* **367**:51-59. DOI: https://doi.org/10.1126/science.aax4735. PMID: 31896710

Cerqueira GC, Cheeseman IH, Schaffner SF, Nair S, McDew-White M, Phyo AP, Ashley EA, Melnikov A, Rogov P, Birren BW, Nosten F, Anderson TJC, Neafsey DE. 2017. Longitudinal genomic surveillance of *Plasmodium falciparum* malaria parasites reveals complex genomic architecture of emerging artemisinin resistance. *Genome Biol* **18**:78. DOI: https://doi.org/10.1186/s13059-017-1204-4. PMID: 28454557

690 Conrad MD, Rosenthal PJ. 2019. Antimalarial drug resistance in Africa: the calm before the storm? *Lancet Infect*
691 *Dis* **19**:e338-e351. DOI: https://doi.org/10.1016/S1473-3099(19)30261-0. PMID: 31375467
692 Das S, Manna S, Saha B, Hati AK, Roy S. 2019. Novel *pfkelch13* gene polymorphism associates with
693 artemisinin resistance in Eastern India. *Clin Infect Dis* **69**:1144-1152. DOI:
694 https://doi.org/10.1093/cid/ciy1038. PMID: 30535043
695 Demas AR, Sharma AI, Wong W, Early AM, Redmond S, Bopp S, Neafsey DE, Volkman SK, Hartl DL, Wirth
696 DF. 2018. Mutations in *Plasmodium falciparum* actin-binding protein coronin confer reduced artemisinin
697 susceptibility. *Proc Natl Acad Sci USA* **115**:12799-12804. DOI:
698 https://doi.org/10.1073/pnas.1812317115. PMID: 30420498
699 Dhingra SK, Small-Saunders JL, Menard D, Fidock DA. 2019. *Plasmodium falciparum* resistance to piperaquine
700 driven by PfCRT. *Lancet Infect Dis* **19**:1168-1169. DOI: https://doi.org/10.1016/S1473-3099(19)30543-
701 2. PMID: 31657776
702 Dondorp AM, Nosten F, Yi P, Das D, Phyo AP, Tarning J, Lwin KM, Ariey F, Hanpithakpong W, Lee SJ,
703 Ringwald P, Silamut K, Imwong M, Chotivanich K, Lim P, Herdman T, An SS, Yeung S, Singhasivanon
704 P, Day NP, Lindegardh N, Socheat D, White NJ. 2009. Artemisinin resistance in *Plasmodium falciparum*
705 malaria. *N Engl J Med* **361**:455-467. DOI: https://doi.org/10.1056/NEJMoa0808859. PMID: 19641202
706 Eastman RT, Fidock DA. 2009. Artemisinin-based combination therapies: a vital tool in efforts to eliminate
707 malaria. *Nat Rev Microbiol* **7**:864-874. DOI: https://doi.org/10.1038/nrmicro2239. PMID: 19881520
708 Frosch AE, Laufer MK, Mathanga DP, Takala-Harrison S, Skarbinski J, Claassen CW, Dzinjalamala FK, Plowe
709 CV. 2014. Return of widespread chloroquine-sensitive *Plasmodium falciparum* to Malawi. *J Infect Dis*
710 **210**:1110-1114. DOI: https://doi.org/10.1093/infdis/jiu216. PMID: 24723474
711 Ghorbal M, Gorman M, Macpherson CR, Martins RM, Scherf A, Lopez-Rubio JJ. 2014. Genome editing in the
712 human malaria parasite *Plasmodium falciparum* using the CRISPR-Cas9 system. *Nat Biotechnol*
713 **32**:819-821. DOI: https://doi.org/10.1038/nbt.2925. PMID: 24880488
714 Gnadig NF, Stokes BH, Edwards RL, Kalantarov GF, Heimsch KC, Kuderjavy M, Crane A, Lee MCS, Straimer
715 J, Becker K, Trakht IN, Odom John AR, Mok S, Fidock DA. 2020. Insights into the intracellular
716 localization, protein associations and artemisinin resistance properties of *Plasmodium falciparum* K13.
717 *PLoS Pathog* **16**:e1008482. DOI: https://doi.org/10.1371/journal.ppat.1008482. PMID: 32310999
718 WWARN K13 Genotype-Phenotype Study Group. 2019. Association of mutations in the *Plasmodium falciparum*
719 Kelch13 gene (Pf3D7_1343700) with parasite clearance rates after artemisinin-based treatments—a
720 WWARN individual patient data meta-analysis. *BMC Med* **17**:1. DOI: https://doi.org/10.1186/s12916-
721 018-1207-3. PMID: 30651111
722 Haldar K, Bhattacharjee S, Safeukui I. 2018. Drug resistance in *Plasmodium*. *Nat Rev Microbiol* **16**:156-170.
723 DOI: https://doi.org/10.1038/nrmicro.2017.161. PMID: 29355852
724 Hanboonkunupakarn B, White NJ. 2020. Advances and roadblocks in the treatment of malaria. *Br J Clin*
725 *Pharmacol* **Jul 12.** DOI: https://doi.org/10.1111/bcp.14474. PMID: 32656850
726 Henrici RC, van Schalkwyk DA, Sutherland CJ. 2019. Modification of *pfap2mu* and *pfubp1* markedly reduces
727 ring-stage susceptibility of *Plasmodium falciparum* to artemisinin *in vitro*. *Antimicrob Agents Chemother*
728 **64**. DOI: https://doi.org/10.1128/AAC.01542-19. PMID: 31636063
729 Henriques G, Hallett RL, Beshir KB, Gadalla NB, Johnson RE, Burrow R, van Schalkwyk DA, Sawa P, Omar
730 SA, Clark TG, Bousema T, Sutherland CJ. 2014. Directional selection at the *pfmdr1*, *pfcrt*, *pfubp1*, and
731 *pfap2mu* loci of *Plasmodium falciparum* in Kenyan children treated with ACT. *J Infect Dis* **210**:2001-
732 2008. DOI: https://doi.org/10.1093/infdis/jiu358. PMID: 24994911
733 Imwong M, Dhorda M, Myo Tun K, Thu AM, Phyo AP, Proux S, Suwannasin K, Kunasol C, Srisutham S,
734 Duanguppama J, Vongpromek R, Promnarate C, Saejeng A, Khantikul N, Sugaram R,
735 Thanapongpichat S, Sawangjaroen N, Sutawong K, Han KT, Htut Y, Linn K, Win AA, Hlaing TM, van
736 der Pluijm RW, Mayxay M, Pongvongsa T, Phommasone K, Tripura R, Peto TJ, von Seidlein L, Nguon
737 C, Lek D, Chan XHS, Rekol H, Leang R, Huch C, Kwiatkowski DP, Miotto O, Ashley EA, Kyaw MP,
738 Pukrittayakamee S, Day NPJ, Dondorp AM, Smithuis FM, Nosten FH, White NJ. 2020. Molecular
739 epidemiology of resistance to antimalarial drugs in the Greater Mekong subregion: an observational
740 study. *Lancet Infect Dis* **20**:1470-1480. DOI: https://doi.org/10.1016/S1473-3099(20)30228-0. PMID:
741 32679084
742 Imwong M, Suwannasin K, Kunasol C, Sutawong K, Mayxay M, Rekol H, Smithuis FM, Hlaing TM, Tun KM, van
743 der Pluijm RW, Tripura R, Miotto O, Menard D, Dhorda M, Day NPJ, White NJ, Dondorp AM. 2017. The
744 spread of artemisinin-resistant *Plasmodium falciparum* in the Greater Mekong subregion: a molecular
745 epidemiology observational study. *Lancet Infect Dis* **17**:491-497. DOI: https://doi.org/10.1016/S1473-
746 3099(17)30048-8. PMID: 28161569

Kayiba NK, Yobi DM, Tshibangu-Kabamba E, Tuan VP, Yamaoka Y, Devleesschauwer B, Mvumbi DM, Okitolonda Wemakoy E, De Mol P, Mvumbi GL, Hayette MP, Rosas-Aguirre A, Speybroeck N. 2020. Spatial and molecular mapping of Pfkelch13 gene polymorphism in Africa in the era of emerging *Plasmodium falciparum* resistance to artemisinin: a systematic review. *Lancet Infect Dis* **21**:e82-e92. DOI: https://doi.org/10.1016/S1473-3099(20)30493-X. PMID: 33125913

Kublin JG, Cortese JF, Njunju EM, Mukadam RA, Wirima JJ, Kazembe PN, Djimde AA, Kouriba B, Taylor TE, Plowe CV. 2003. Reemergence of chloroquine-sensitive *Plasmodium falciparum* malaria after cessation of chloroquine use in Malawi. *J Infect Dis* **187**:1870-1875. DOI: https://doi.org/10.1086/375419. PMID: 12792863

Laufer MK, Thesing PC, Eddington ND, Masonga R, Dzinjalamala FK, Takala SL, Taylor TE, Plowe CV. 2006. Return of chloroquine antimalarial efficacy in Malawi. *N Engl J Med* **355**:1959-1966. DOI: https://doi.org/10.1056/NEJMoa062032. PMID: 17093247

Lim MY, LaMonte G, Lee MCS, Reimer C, Tan BH, Corey V, Tjahjadi BF, Chua A, Nachon M, Wintjens R, Gedeck P, Malleret B, Renia L, Bonamy GMC, Ho PC, Yeung BKS, Chow ED, Lim L, Fidock DA, Diagana TT, Winzeler EA, Bifani P. 2016. UDP-galactose and acetyl-CoA transporters as *Plasmodium* multidrug resistance genes. *Nat Microbiol* **1**:16166. DOI: https://doi.org/10.1038/nmicrobiol.2016.166. PMID: 27642791

Lu F, Culleton R, Zhang M, Ramaprasad A, von Seidlein L, Zhou H, Zhu G, Tang J, Liu Y, Wang W, Cao Y, Xu S, Gu Y, Li J, Zhang C, Gao Q, Menard D, Pain A, Yang H, Zhang Q, Cao J. 2017. Emergence of indigenous artemisinin-resistant *Plasmodium falciparum* in Africa. *N Engl J Med* **376**:991-993. DOI: https://doi.org/10.1056/NEJMc1612765. PMID: 28225668

MalariaGEN *Plasmodium falciparum* Community Project. 2016. Genomic epidemiology of artemisinin resistant malaria. *eLife* **5**:e08714. DOI: https://doi.org/10.7554/eLife.08714. PMID: 26943619

Mathieu LC, Cox H, Early AM, Mok S, Lazrek Y, Paquet JC, Ade MP, Lucchi NW, Grant Q, Udhayakumar V, Alexandre JS, Demar M, Ringwald P, Neafsey DE, Fidock DA, Musset L. 2020. Local emergence in Amazonia of *Plasmodium falciparum* k13 C580Y mutants associated with *in vitro* artemisinin resistance. *eLife* **9**:e51015. DOI: https://doi.org/10.7554/eLife.51015. PMID: 32394893

Menard D, Khim N, Beghain J, Adegnika AA, Shafiul-Alam M, Amodu O, Rahim-Awab G, Barnadas C, Berry A, Boum Y, Bustos MD, Cao J, Chen JH, Collet L, Cui L, Thakur GD, Dieye A, Djalle D, Dorkenoo MA, Eboumbou-Moukoko CE, Espino FE, Fandeur T, Ferreira-da-Cruz MF, Fola AA, Fuehrer HP, Hassan AM, Herrera S, Hongvanthong B, Houze S, Ibrahim ML, Jahirul-Karim M, Jiang L, Kano S, Ali-Khan W, Khanthavong M, Kremsner PG, Lacerda M, Leang R, Leelawong M, Li M, Lin K, Mazarati JB, Menard S, Morlais I, Muhindo-Mavoko H, Musset L, Na-Bangchang K, Nambozi M, Niare K, Noedl H, Ouedraogo JB, Pillai DR, Pradines B, Quang-Phuc B, Ramharter M, Randrianarivelojosia M, Sattabongkot J, Sheikh-Omar A, Silue KD, Sirima SB, Sutherland C, Syafruddin D, Tahar R, Tang LH, Toure OA, Tshibangu-wa-Tshibangu P, Vigan-Womas I, Warsame M, Wini L, Zakeri S, Kim S, Eam R, Berne L, Khean C, Chy S, Ken M, Loch K, Canier L, Duru V, Legrand E, Barale JC, Stokes B, Straimer J, Witkowski B, Fidock DA, Rogier C, Ringwald P, Ariey F, Mercereau-Puijalon O, Karma Consortium. 2016. A worldwide map of *Plasmodium falciparum* K13-propeller polymorphisms. *N Engl J Med* **374**:2453-2464. DOI: https://doi.org/10.1056/NEJMoa1513137. PMID: 27332904

Miotto O, Amato R, Ashley EA, MacInnis B, Almagro-Garcia J, Amaratunga C, Lim P, Mead D, Oyola SO, Dhorda M, Imwong M, Woodrow C, Manske M, Stalker J, Drury E, Campino S, Amenga-Etego L, Thanh TN, Tran HT, Ringwald P, Bethell D, Nosten F, Phyo AP, Pukrittayakamee S, Chotivanich K, Chuor CM, Nguon C, Suon S, Sreng S, Newton PN, Mayxay M, Khanthavong M, Hongvanthong B, Htut Y, Han KT, Kyaw MP, Faiz MA, Fanello CI, Onyamboko M, Mokuolu OA, Jacob CG, Takala-Harrison S, Plowe CV, Day NP, Dondorp AM, Spencer CC, McVean G, Fairhurst RM, White NJ, Kwiatkowski DP. 2015. Genetic architecture of artemisinin-resistant *Plasmodium falciparum*. *Nat Genet* **47**:226-234. DOI: https://doi.org/10.1038/ng.3189. PMID: 25599401

Miotto O, Sekihara M, Tachibana SI, Yamauchi M, Pearson RD, Amato R, Goncalves S, Mehra S, Noviyanti R, Marfurt J, Auburn S, Price RN, Mueller I, Ikeda M, Mori T, Hirai M, Tavul L, Hetzel MW, Laman M, Barry AE, Ringwald P, Ohashi J, Hombhanje F, Kwiatkowski DP, Mita T. 2020. Emergence of artemisinin-resistant *Plasmodium falciparum* with *kelch13* C580Y mutations on the island of New Guinea. *PLoS Pathog* **16**:e1009133. DOI: https://doi.org/10.1371/journal.ppat.1009133. PMID: 33320907

Mok S, Stokes BH, Gnadig NF, Ross LS, Yeo T, Amaratunga C, Allman E, Solyakov L, Bottrill AR, Tripathi J, Fairhurst RM, Llinas M, Bozdech Z, Tobin AB, Fidock DA. 2021. Artemisinin-resistant K13 mutations rewire *Plasmodium falciparum*'s intra-erythrocytic metabolic program to enhance survival. *Nat Commun* **12**:530. DOI: https://doi.org/10.1038/s41467-020-20805-w. PMID: 33483501

Nair S, Li X, Arya GA, McDew-White M, Ferrari M, Nosten F, Anderson TJC. 2018. Do fitness costs explain the rapid spread of *kelch13*-C580Y substitutions conferring artemisinin resistance? *Antimicrob Agents Chemother* **62**:e00605-00618. DOI: https://doi.org/10.1128/AAC.00605-18. PMID: 29914963

Noedl H, Se Y, Schaecher K, Smith BL, Socheat D, Fukuda MM, Artemisinin Resistance in Cambodia 1 (ARC1) Study Consortium. 2008. Evidence of artemisinin-resistant malaria in western Cambodia. *N Engl J Med* **359**:2619-2620. DOI: https://doi.org/10.1056/NEJMc0805011. PMID: 19064625

Noedl H, Socheat D, Satimai W. 2009. Artemisinin-resistant malaria in Asia. *N Engl J Med* **361**:540-541. DOI: https://doi.org/10.1056/NEJMc0900231. PMID: 19641219

Ord R, Alexander N, Dunyo S, Hallett R, Jawara M, Targett G, Drakeley CJ, Sutherland CJ. 2007. Seasonal carriage of *pfcrt* and *pfmdr1* alleles in Gambian *Plasmodium falciparum* imply reduced fitness of chloroquine-resistant parasites. *J Infect Dis* **196**:1613-1619. DOI: https://doi.org/10.1086/522154. PMID: 18008244

Phyo AP, Ashley EA, Anderson TJC, Bozdech Z, Carrara VI, Sriprawat K, Nair S, White MM, Dziekan J, Ling C, Proux S, Konghahong K, Jeeyapant A, Woodrow CJ, Imwong M, McGready R, Lwin KM, Day NPJ, White NJ, Nosten F. 2016. Declining efficacy of artemisinin combination therapy against *P. falciparum* malaria on the Thai-Myanmar border (2003-2013): The role of parasite genetic factors. *Clin Infect Dis* **63**:784-791. DOI: https://doi.org/10.1093/cid/ciw388. PMID: 27313266

Ross LS, Dhingra SK, Mok S, Yeo T, Wicht KJ, Kumpornsin K, Takala-Harrison S, Witkowski B, Fairhurst RM, Ariey F, Menard D, Fidock DA. 2018. Emerging Southeast Asian PfCRT mutations confer *Plasmodium falciparum* resistance to the first-line antimalarial piperaquine. *Nat Commun* **9**:3314. DOI: https://doi.org/10.1038/s41467-018-05652-0. PMID: 30115924

Schmedes SE, Patel D, Dhal S, Kelley J, Svigel SS, Dimbu PR, Adeothy AL, Kahunu GM, Nkoli PM, Beavogui AH, Kariuki S, Mathanga DP, Koita O, Ishengoma D, Mohamad A, Hawela M, Moriarty LF, Samuels AM, Gutman J, Plucinski MM, Udhayakumar V, Zhou Z, Lucchi NW, Venkatesan M, Halsey ES, Talundzic E. 2021. *Plasmodium falciparum kelch 13* Mutations, 9 Countries in Africa, 2014-2018. *Emerg Infect Dis* **27**:1902-1908. DOI: https://doi.org/10.3201/eid2707.203230. PMID: 34152946

Sherrard-Smith E, Hogan AB, Hamlet A, Watson OJ, Whittaker C, Winskill P, Ali F, Mohammad AB, Uhomoibhi P, Maikore I, Ogbulafor N, Nikau J, Kont MD, Challenger JD, Verity R, Lambert B, Cairns M, Rao B, Baguelin M, Whittles LK, Lees JA, Bhatia S, Knock ES, Okell L, Slater HC, Ghani AC, Walker PGT, Okoko OO, Churcher TS. 2020. The potential public health consequences of COVID-19 on malaria in Africa. *Nat Med* **26**:1411-1416. DOI: https://doi.org/10.1038/s41591-020-1025-y. PMID: 32770167

Siddiqui FA, Boonhok R, Cabrera M, Mbenda HGN, Wang M, Min H, Liang X, Qin J, Zhu X, Miao J, Cao Y, Cui L. 2020. Role of *Plasmodium falciparum* Kelch 13 protein mutations in *P. falciparum* populations from northeastern Myanmar in mediating artemisinin resistance. *mBio* **11**:e01134-01119. DOI: https://doi.org/10.1128/mBio.01134-19. PMID: 32098812

Siddiqui G, Srivastava A, Russell AS, Creek DJ. 2017. Multi-omics based identification of specific biochemical changes associated with PfKelch13-mutant artemisinin-resistant *Plasmodium falciparum*. *J Infect Dis* **215**:1435-1444. DOI: https://doi.org/10.1093/infdis/jix156. PMID: 28368494

Straimer J, Gnadig NF, Stokes BH, Ehrenberger M, Crane AA, Fidock DA. 2017. *Plasmodium falciparum* K13 mutations differentially impact ozonide susceptibility and parasite fitness *in vitro*. *mBio* **8**:e00172-00117. DOI: https://doi.org/10.1128/mBio.00172-17. PMID: 28400526

Straimer J, Gnadig NF, Witkowski B, Amaratunga C, Duru V, Ramadani AP, Dacheux M, Khim N, Zhang L, Lam S, Gregory PD, Urnov FD, Mercereau-Puijalon O, Benoit-Vical F, Fairhurst RM, Menard D, Fidock DA. 2015. K13-propeller mutations confer artemisinin resistance in *Plasmodium falciparum* clinical isolates. *Science* **347**:428-431. DOI: https://doi.org/10.1126/science.1260867. PMID: 25502314

Sutherland CJ, Henrici RC, Artavanis-Tsakonas K. 2020. Artemisinin susceptibility in the malaria parasite *Plasmodium falciparum*: propellers, adaptor proteins and the need for cellular healing. *FEMS Microbiol Rev*. DOI: https://doi.org/10.1093/femsre/fuaa056. PMID: 33095255

Uwimana A, Legrand E, Stokes BH, Ndikumana JM, Warsame M, Umulisa N, Ngamije D, Munyaneza T, Mazarati JB, Munguti K, Campagne P, Criscuolo A, Ariey F, Murindahabi M, Ringwald P, Fidock DA, Mbituyumuremyi A, Menard D. 2020. Emergence and clonal expansion of *in vitro* artemisinin-resistant *Plasmodium falciparum kelch13* R561H mutant parasites in Rwanda. *Nature Med* **26**:1602-1608. DOI: https://doi.org/10.1038/s41591-020-1005-2. PMID: 32747827

Uwimana A, Umulisa N, Venkatesan M, Svigel SS, Zhou Z, Munyaneza T, Habimana RM, Rucogoza A, Moriarty LF, Sandford R, Piercefield E, Goldman I, Ezema B, Talundzic E, Pacheco MA, Escalante AA, Ngamije D, Mangala JN, Kabera M, Munguti K, Murindahabi M, Brieger W, Musanabaganwa C, Mutesa L, Udhayakumar V, Mbituyumuremyi A, Halsey ES, Lucchi NW. 2021. Association of *Plasmodium*

falciparum kelch13 R561H genotypes with delayed parasite clearance in Rwanda: an open-label, single-arm, multicentre, therapeutic efficacy study. *Lancet Infect Dis*. DOI: https://doi.org/10.1016/S1473-3099(21)00142-0. PMID: 33864801

van der Pluijm RW, Imwong M, Chau NH, Hoa NT, Thuy-Nhien NT, Thanh NV, Jittamala P, Hanboonkunupakarn B, Chutasmit K, Saelow C, Runjarern R, Kaewmok W, Tripura R, Peto TJ, Yok S, Suon S, Sreng S, Mao S, Oun S, Yen S, Amaratunga C, Lek D, Huy R, Dhorda M, Chotivanich K, Ashley EA, Mukaka M, Waithira N, Cheah PY, Maude RJ, Amato R, Pearson RD, Goncalves S, Jacob CG, Hamilton WL, Fairhurst RM, Tarning J, Winterberg M, Kwiatkowski DP, Pukrittayakamee S, Hien TT, Day NP, Miotto O, White NJ, Dondorp AM. 2019. Determinants of dihydroartemisinin-piperaquine treatment failure in *Plasmodium falciparum* malaria in Cambodia, Thailand, and Vietnam: a prospective clinical, pharmacological, and genetic study. *Lancet Infect Dis* **19**:952-961. DOI: https://doi.org/10.1016/S1473-3099(19)30391-3. PMID: 31345710

Vaughan AM, Pinapati RS, Cheeseman IH, Camargo N, Fishbaugher M, Checkley LA, Nair S, Hutyra CA, Nosten FH, Anderson TJ, Ferdig MT, Kappe SH. 2015. *Plasmodium falciparum* genetic crosses in a humanized mouse model. *Nat Methods* **12**:631-633. DOI: https://doi.org/10.1038/nmeth.3432. PMID: 26030447

White J, Dhingra SK, Deng X, El Mazouni F, Lee MCS, Afanador GA, Lawong A, Tomchick DR, Ng CL, Bath J, Rathod PK, Fidock DA, Phillips MA. 2019. Identification and mechanistic understanding of dihydroorotate dehydrogenase point mutations in *Plasmodium falciparum* that confer *in vitro* resistance to the clinical candidate DSM265. *ACS Infect Dis* **5**:90-101. DOI: https://doi.org/10.1021/acsinfecdis.8b00211. PMID: 30375858

White NJ, Pukrittayakamee S, Hien TT, Faiz MA, Mokuolu OA, Dondorp AM. 2014. Malaria. *Lancet* **383**:723-735. DOI: https://doi.org/10.1016/S0140-6736(13)60024-0. PMID: 23953767

WHO. 2019. WHO status report on artemisinin resistance and ACT efficacy. https://www.who.int/docs/default-source/documents/publications/gmp/who-cds-gmp-2019-17-eng.pdf?ua=1.

WHO. 2020. World malaria report 2020. https://www.who.int/teams/global-malaria-programme/reports/world-malaria-report-2020.

Wicht KJ, Mok S, Fidock DA. 2020. Molecular mechanisms of drug resistance in *Plasmodium falciparum* malaria. *Annu Rev Microbiol* **74**:431-454. DOI: https://doi.org/10.1146/annurev-micro-020518-115546. PMID: 32905757

Witkowski B, Amaratunga C, Khim N, Sreng S, Chim P, Kim S, Lim P, Mao S, Sopha C, Sam B, Anderson JM, Duong S, Chuor CM, Taylor WR, Suon S, Mercereau-Puijalon O, Fairhurst RM, Menard D. 2013. Novel phenotypic assays for the detection of artemisinin-resistant *Plasmodium falciparum* malaria in Cambodia: *in-vitro* and *ex-vivo* drug-response studies. *Lancet Infect Dis* **13**:1043-1049. DOI: https://doi.org/10.1016/S1473-3099(13)70252-4. PMID: 24035558

Witkowski B, Lelievre J, Barragan MJ, Laurent V, Su XZ, Berry A, Benoit-Vical F. 2010. Increased tolerance to artemisinin in *Plasmodium falciparum* is mediated by a quiescence mechanism. *Antimicrob Agents Chemother* **54**:1872-1877. DOI: https://doi.org/10.1128/AAC.01636-09. PMID: 20160056

Witmer K, Dahalan FA, Delves MJ, Yahiya S, Watson OJ, Straschil U, Chiwcharoen D, Sornboon B, Pukrittayakamee S, Pearson RD, Howick VM, Lawniczak MKN, White NJ, Dondorp AM, Okell LC, Chotivanich K, Ruecker A, Baum J. 2020. Transmission of artemisinin-resistant malaria parasites to mosquitoes under antimalarial drug pressure. *Antimicrob Agents Chemother* **65**. DOI: https://doi.org/10.1128/AAC.00898-20. PMID: 33139275

Xi R, Hadjipanayis AG, Luquette LJ, Kim TM, Lee E, Zhang J, Johnson MD, Muzny DM, Wheeler DA, Gibbs RA, Kucherlapati R, Park PJ. 2011. Copy number variation detection in whole-genome sequencing data using the Bayesian information criterion. *Proc Natl Acad Sci USA* **108**:E1128-1136. DOI: https://doi.org/10.1073/pnas.1110574108. PMID: 22065754

Xiong A, Prakash P, Gao X, Chew M, Tay IJJ, Woodrow CJ, Engelward BP, Han J, Preiser PR. 2020. K13-mediated reduced susceptibility to artemisinin in *Plasmodium falciparum* is overlaid on a trait of enhanced DNA damage repair. *Cell Rep* **32**:107996. DOI: https://doi.org/10.1016/j.celrep.2020.107996. PMID: 32755588

Yang T, Yeoh LM, Tutor MV, Dixon MW, McMillan PJ, Xie SC, Bridgford JL, Gillett DL, Duffy MF, Ralph SA, McConville MJ, Tilley L, Cobbold SA. 2019. Decreased K13 abundance reduces hemoglobin catabolism and proteotoxic stress, underpinning artemisinin resistance. *Cell Rep* **29**:2917-2928 e2915. DOI: https://doi.org/10.1016/j.celrep.2019.10.095. PMID: 31775055

Legends

Figure 1. Frequency and distribution of *K13* alleles in 11 African countries.

Map of Africa with pie charts representing the proportions of sequenced samples per country that harbor the K13 wild-type sequence (3D7 reference), the R561H variant (the most commonly identified mutation, unique to Rwanda; see inset), or another less frequent non-synonymous K13 mutation. Sample sizes and years of sample collection are indicated. Mutations and numbers of African samples sequenced per country, and prior citations as appropriate, are listed in **Figure 1–source data 1**.

Figure 1–source data 1. Distribution of *K13* alleles over time in African countries (2011-2019).

Figure 2. Gene-edited mutant K13 African parasites display variable levels of RSA survival.

(A-D) RSA survival rates for (A) 3D7 (Africa), (B) F32 (Tanzania), (C) UG659 (Uganda), or (D) UG815 (Uganda) K13 wild-type parental lines and CRISPR/Cas9-edited K13 R561H, M579I or C580Y mutant clones. Unedited parental lines are described in **Table 1** and **Supplementary file 4**. For 3D7, we also included a K13 wild-type control (ctrl) line harboring silent shield mutations at the K13 gRNA cut site. Results show the percentage of early ring-stage parasites (0-3 h post invasion) that survived a 6 h pulse of 700 nM DHA, relative to DMSO-treated parasites assayed in parallel. Percent survival values are shown as means ± SEM (detailed in **Figure 2–source data 1**). Results were obtained from 3 to 8 independent experiments, each performed in duplicate. *P* values were determined by unpaired *t* tests and were calculated for mutant lines relative to the isogenic line expressing wild-type *K13*. ** $P<0.01$; *** $P<0.001$; **** $P<0.0001$.

Figure 2–source data 1. Ring-stage survival (RSA) assay data for K13 edited African parasites and controls.

Figure 2–figure supplement 1. African K13 mutations result in reduced K13 protein levels in 3D7 parasites.

(A) Representative Western blot of parasite extracts probed with an anti-K13 monoclonal antibody (clone E9) that recognizes full-length K13 (~85 kDa) and lower molecular weight bands, presumably N-terminal

degradation products, as previously reported (Gnadig *et al.*, 2020). Tightly synchronized K13 wild-type, R561H, M579I or C580Y 3D7 parasites were harvested as 0-6 h ring stages. ERD2 was used as a loading control. Experiments were performed on three independent occasions. (B) Quantification of K13 mutant protein levels versus K13 wild-type protein levels across independent replicates, performed using ImageJ, with all protein levels normalized to the ERD2 loading control. Western blots revealed reduced levels of K13 protein in the three mutant lines relative to wild-type 3D7 parasites. Results are shown as means ± SEM. WT, wild-type.

Figure 2–figure supplement 1–source data 1. Raw figure files for K13 Western blots performed on 3D7 parasites.

Figure 3. K13 mutations cause differential impacts on *in vitro* growth rates across gene-edited African strains.

(A-D) Percentage of mutant allele relative to the wild-type allele over time in (A) 3D7, (B) F32, (C) UG659, and (D) UG815 parasite cultures in which K13 mutant clones were co-cultured at 1:1 starting ratios with isogenic K13 wild-type controls over a period of 36 days. Results, shown as means ± SEM, were obtained from 2 to 5 independent experiments, each performed in duplicate. Values are provided in **Figure 3–source data 1**. (E) The percent reduction in growth rate per 48 h generation, termed the fitness cost, is presented as mean ± SEM for each mutant line relative to its isogenic wild-type comparator. (F) Fitness costs for mutant lines and isogenic wild-type comparators plotted relative to RSA survival values for the same lines.

Figure 3–source data 1. Fitness assay data for *K13* edited African parasite lines and controls.

Figure 4. The *K13* C580Y allele has progressively outcompeted all other alleles in Cambodia.

(A-D) Stacked bar charts representing the percentage of sequenced samples expressing the *K13* wild-type allele or individual variants, calculated based on the total number of samples (listed in parentheses) for a given period. Sample collection was segregated into four regions in Cambodia (detailed in **Figure 4–figure supplement 1**). All K13 mutant samples harbored a single non-synonymous nucleotide polymorphism. Mutations and numbers of Cambodian samples sequenced per region/year, including prior citations as appropriate, are listed in **Figure 4–source data 1**.

Figure 4–source data 1. Distribution of *K13* alleles over time in Cambodia (2001-2017).

Figure 4–figure supplement 1. Regions of sample collection in Cambodia for K13 sequencing.

Map depicting the four regions of Cambodia (western, northern, eastern, and southern) in which samples were collected between 2001 and 2017 for K13 genotyping. Genotyping data are presented in **Figure 4**.

Figure 5. Southeast Asian K13 mutations yield elevated RSA survival and minor impacts on *in vitro* growth in gene-edited parasite lines.

(A, B) RSA survival rates for Dd2 (Indochina) and Cam3.II (Cambodia) *P. falciparum* parasites expressing wild-type or mutant K13. Gene-edited parasites were generated using CRISPR/Cas9 or zinc-finger nucleases. Control (ctrl) lines express silent shield mutations at the *K13* gRNA cut site. Parental lines are described in **Table 1** and **Supplementary file 4**. Results show the percentage of early ring-stage parasites (0-3 h post invasion) that survived a 6 h pulse of 700 nM DHA, relative to DMSO-treated parasites processed in parallel. Percent survival values are shown as means ± SEM (detailed in **Figure 5–source data 1**). Results were obtained from 3 to 13 independent experiments, each performed in duplicate. *P* values were determined by unpaired *t* tests and were calculated for mutant lines relative to the isogenic line expressing wild-type *K13*. *** $P<0.001$; **** $P<0.0001$. (C) Percent reductions in growth rate per 48 h generation, expressed as the fitness cost, for each Dd2 mutant line relative to the $Dd2^{WT}$ line. Fitness costs were determined by co-culturing a $Dd2^{eGFP}$ reporter line with either the Dd2 K13 wild-type parental line ($Dd2^{WT}$) or gene-edited K13 mutant lines. Co-cultures were maintained for 20 days and percentages of $eGFP^{+}$ parasites were determined by flow cytometry (see **Figure 5–source data 2 and Figure 5–figure supplement 1**). Fitness costs were initially calculated relative to the $Dd2^{eGFP}$ reporter line (**Figure 5–figure supplement 1**) and then normalized to the $Dd2^{WT}$ line. Mean ± SEM values were obtained from three independent experiments, each performed in triplicate. (D) Fitness costs for K13 mutant lines, relative to the $Dd2^{WT}$ line, were plotted against their corresponding RSA survival values.

Figure 5–source data 1. Ring-stage survival (RSA) assay data for *K13* edited SE Asian parasites and controls (Dd2 and Cam3.II strains).

Figure 5–source data 2. Fitness assay data (percent eGFP+ parasites) for *K13* edited Dd2 parasites and parental control.

Figure 5–figure supplement 1. Southeast Asian K13 mutations result in minor in vitro growth defects in Dd2 parasites, with the exception of the C580Y and P553L mutations.

(A) Percentage of $eGFP^{+}$ parasites over time in parasite cultures in which an eGFP-expressing Dd2 line was co-cultured in a 1:1 mixture with either the Dd2 K13 WT parental line ($Dd2^{WT}$) or individual Dd2 gene-edited K13 mutant lines. Co-cultures were maintained over a period of 20 days, and the percentage of $eGFP^{+}$ parasites in each mix was determined by flow cytometry. Data are shown as means ± SEM. Results were obtained from three independent experiments, each performed in triplicate. (B) Percent reduction in growth rate per 48 h generation, termed the fitness cost, for $Dd2^{WT}$ and K13-edited mutant lines relative to the $Dd2^{eGFP}$ line. Results are shown as means ± SEM.

Figure 6. Thai isolates expressing mutant K13 display variable RSA survival rates.

RSA survival rates for (A-E) *K13*-edited Thai isolates and (F) K13 E252Q unedited Thai lines, shown as means ± SEM (detailed in **Figure 6–source data 1**). Results were obtained from 3 to 7 independent experiments, each performed in duplicate. *P* values were determined by unpaired *t* tests and were calculated for mutant lines relative to the isogenic line expressing wild-type *K13*. * $P<0.05$; ** $P<0.01$; *** $P<0.001$.

Figure 6–source data 1. Ring-stage survival (RSA) assay data for *K13* edited Thai parasites and controls.

Figure 7. Ferredoxin (fd) and multidrug resistance protein 2 (mdr2) mutations do not impact RSA survival or *in vitro* growth rates in K13 C580Y parasites.

RSA survival rates for (A) $RF7^{C580Y}$ parasite lines expressing the fd variant D193Y (parent), this variant plus silent shield mutations (edited control), or fd D193 (edited revertant), and (C) $Cam3.II^{C580Y}$ parasite lines expressing the mdr2 variant T484I (parent), this variant plus silent shield mutations (edited control), or mdr2

T484 (edited revertant). Parental lines are described in **Table 1** and **Supplementary file 4**. Mean ± SEM survival rates were generated from three independent experiments, each performed in duplicate. (B, D) *In vitro* eGFP-based fitness assays performed with (B) *fd* and (D) *mdr2* RF7^{C580Y} or Cam3.II^{C580Y} edited lines, respectively. Competitive growth assays were seeded with individual lines plus the Dd2^{eGFP} reporter line at a 10:1 starting ratio. Results show the percentage of eGFP^{+} parasites over time. Co-cultures were maintained over a period of 24 days (*fd*-edited lines) or 30 days (*mdr2*-edited lines) and percentages of eGFP^{+} parasites were determined by flow cytometry. Results were obtained from 2-3 independent experiments, each performed in triplicate, and are shown as means ± SEM. All values are provided in **Figure 7–source data 1–3**.

Figure 7–source data 1. Ring-stage survival (RSA) assay data for fd and mdr2 edited parasites and controls.

Figure 7–source data 2. Fitness assay data (percent eGFP+ parasites) for RF7 fd edited parasites and parental control.

Figure 7–source data 3. Fitness assay data (percent eGFP+ parasites) for Cam3.II mdr2 edited parasites and parental control.

Figure 7–figure supplement 1. Ferredoxin (fd) and multidrug resistance protein 2 (mdr2) mutations do not impact RSA survival or *in vitro* growth in K13 C580Y parasites.

(A, B) Ring-stage survival assays (RSAs) performed on *fd* and *mdr2* edited lines and parental controls (RF7^{C580Y} and Cam3.II^{C580Y}, respectively). Results show RSA survival rates across a range of DHA concentrations. Survival rates were calculated relative to DMSO-treated parasites processed in parallel. Results were obtained from three independent experiments, each performed in duplicate. Data are shown as means ± SEM. (C, D) *In vitro* eGFP-based fitness assays performed with (C) *fd* and (D) *mdr2* RF7^{C580Y} or Cam3.II^{C580Y} edited lines, respectively. Competitive growth assays were seeded with individual lines plus the Dd2^{eGFP} reporter line at a 100:1 starting ratio. Results show the percentage of eGFP^{+} parasites over time. Co-cultures were maintained over a period of 24 days (*fd*-edited lines) or 30 days (*mdr2*-edited lines) and percentages of eGFP^{+} parasites

were determined by flow cytometry. Results were obtained from 2 to 3 independent experiments, each performed in triplicate, and are shown as means ± SEM.

Supplementary Files

Supplementary file 1. Sample information and approval from within-country ethics committees for K13 genotyping data.

Supplementary file 2. CRISPR/Cas9 strategy for editing the *K13* locus.

All-in-one plasmid approach used for CRISPR/Cas9-mediated *K13* gene editing, consisting of a *K13*-specific donor template for homology-directed repair, a *K13*-specific gRNA expressed from the *U6* promoter, a Cas9 cassette with expression driven by the *calmodulin* (*cam*) promoter, and a selectable marker (human *dhfr*, conferring resistance to the antimalarial WR99210 that inhibits *P. falciparum dhfr*). The Cas9 sequence was codon-optimized for improved expression in P. falciparum. Donors coding for specific mutations of interest (e.g., K13 C580Y, red star) were generated by site-directed mutagenesis of the K13 wild-type donor sequence. Green bars indicate the presence of silent shield mutations that were introduced to protect the edited locus from further cleavage. The lightning bolt indicates the location of the cut site in the genomic target locus. Primers used for cloning and final plasmids are described in **Supplementary files 7** and **8**, respectively.

Supplementary file 3. Crystal structure of K13 propeller domain showing positions of mutated residues.

(A, B) Top and (C, D) side views of the crystal structure of the K13 propeller domain (PDB ID: 4YY8), highlighting residues of interest (F446I, orange; R539T, dark blue; I543T, purple; P553L, pink; R561H, dark turquoise; P574L, light turquoise; M579I medium blue; C580Y, red). Structures shown in (A) and (C) show wild-type residues while (B) and (D) show mutated residues.

Supplementary file 4. Geographic origin and drug resistance genotypes of Plasmodium falciparum clinical isolates and reference lines employed in this study.

Supplementary file 5. Transgenic *Plasmodium falciparum* lines generated in this study.

Supplementary file 6. CRISPR/Cas9 strategy for editing the *ferredoxin* (*fd*) and *multidrug resistance protein 2* (*mdr2*) loci.

All-in-one plasmid approaches used for CRISPR/Cas9-mediated editing of (A) the *ferredoxin* (*fd*) locus or (B) the *multidrug resistance protein 2* (*mdr2*) locus. Plasmids consisted of a *fd* (A) or *mdr2* (B) specific donor template for homology-directed repair, a gene-specific gRNA expressed from the *U6* promoter, a Cas9 cassette with expression driven by the *cam* promoter, and a selectable marker (human *dhfr*, conferring resistance to WR99210). Donors coding for specific mutations of interest (fd D193Y or mdr2 T484I) were generated by site-directed mutagenesis of the wild-type donor sequences. Red bars indicate the presence of silent shield mutations used to protect edited loci from further cleavage. Primers used for cloning and final plasmids are described in **Supplementary files 7** and **8**, respectively.

Supplementary file 7. Oligonucleotides used in this study.

Supplementary file 8. Description of gene-editing plasmids generated in this study.

Supplementary file 9. Real-Time PCR (qPCR) primers and probes used in this study.

1103 **Table 1. *Plasmodium falciparum* lines employed herein.**

Parasite	Origin	Year	*K13*	Resistance
$3D7^{WT}$	Africa	1981	WT	--
$F32^{WT}$	Tanzania	1982	WT	--
$UG659^{WT}$	Uganda	2007	WT	CQ, SP
$UG815^{WT}$	Uganda	2008	WT	CQ, SP
$Dd2^{WT}$	Indochina	1980	WT	CQ, MFQ, SP
$Cam3.II^{WT}$	Cambodia	2010	WT	CQ, SP
$CamWT^{C580Y}$	Cambodia	2010	C580Y	ART, CQ, SP
$RF7^{C580Y}$	Cambodia	2012	C580Y	ART, CQ, PPQ, SP
$Thai1^{WT}$	Thailand	2003	WT	CQ, SP
$Thai2^{WT}$	Thailand	2004	WT	CQ, MFQ, SP
$Thai3^{WT}$	Thailand	2003	WT	CQ, SP
$Thai4^{WT}$	Thailand	2003	WT	CQ, SP
$Thai5^{WT}$	Thailand	2011	WT	CQ, SP
$Thai6^{E252Q}$	Thailand	2008	E252Q	ART (low), CQ, MFQ, SP
$Thai7^{E252Q}$	Thailand	2010	E252Q	ART (low), CQ, MFQ, SP

ART, artemisinin; CQ, chloroquine; MFQ, mefloquine; PPQ, piperaquine; SP, sulfadoxine/pyrimethamine; WT, wild type.

1104

Figure 1

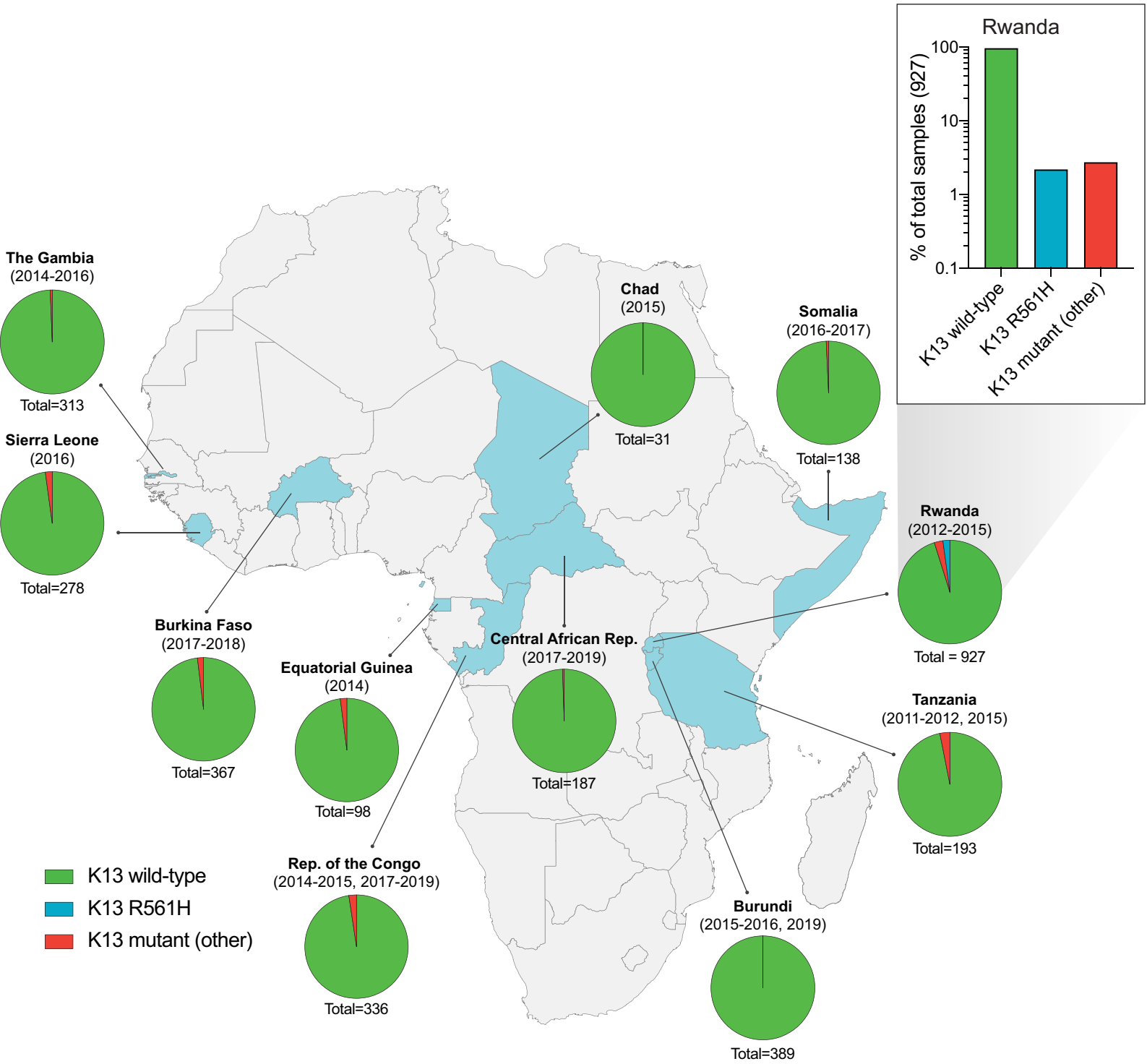
Rwanda
% of total samples (927)
100
10
1
0.1
K13 wild-type
K13 R561H
K13 mutant (other)
The Gambia
(2014-2016)
Total=313
Sierra Leone
(2016)
Total=278
Burkina Faso
(2017-2018)
Total=367
Equatorial Guinea
(2014)
Total=98
Rep. of the Congo
(2014-2015, 2017-2019)
Total=336
Central African Rep.
(2017-2019)
Total=187
Chad
(2015)
Total=31
Somalia
(2016-2017)
Total=138
Rwanda
(2012-2015)
Total = 927
Tanzania
(2011-2012, 2015)
Total=193
Burundi
(2015-2016, 2019)
Total=389
K13 wild-type
K13 R561H
K13 mutant (other)

Figure 2

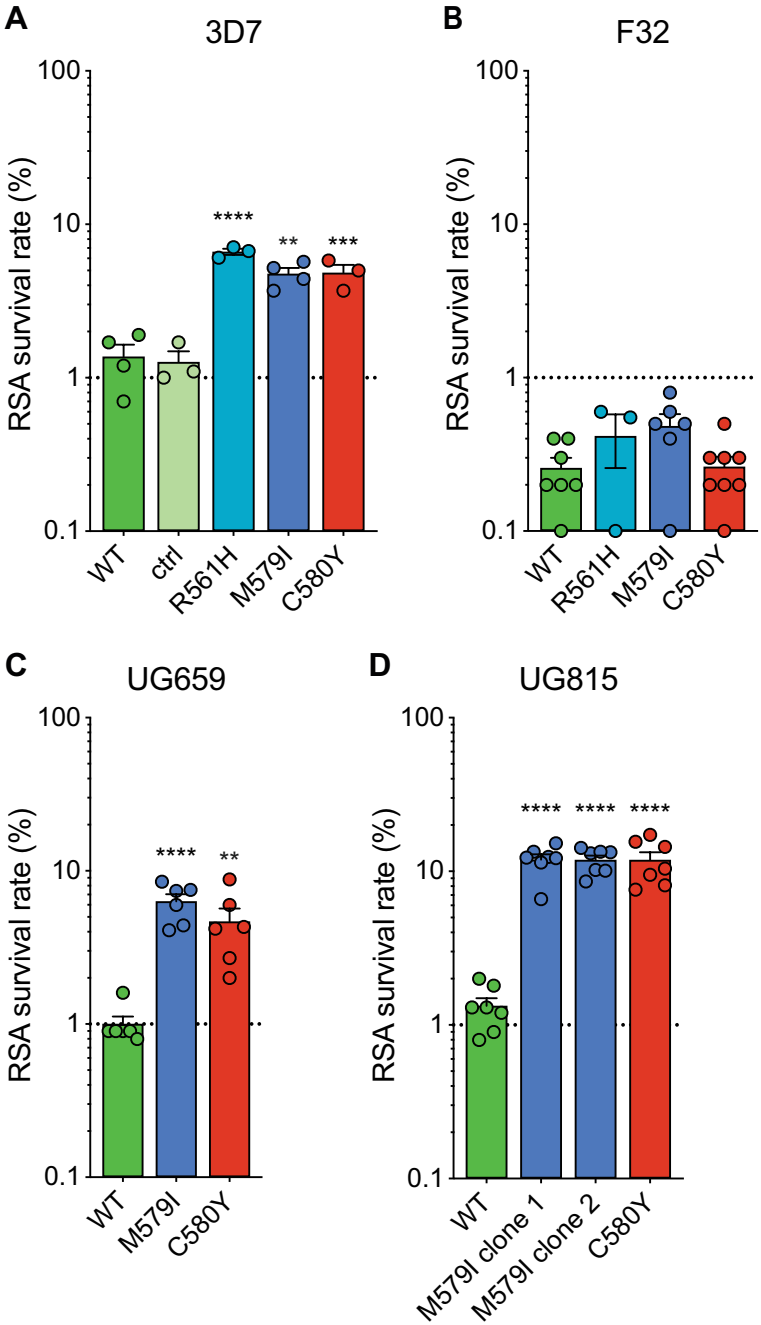
A
3D7
RSA survival rate (%)
100
10
1
0.1
****
**
***
WT
ctrl
R561H
M579I
C580Y
B
F32
RSA survival rate (%)
100
10
1
0.1
WT
R561H
M579I
C580Y
C
UG659
RSA survival rate (%)
100
10
1
0.1
****
**
WT
M579I
C580Y
D
UG815
RSA survival rate (%)
100
10
1
0.1
****
****
****
WT
M579I clone 1
M579I clone 2
C580Y

Figure 3

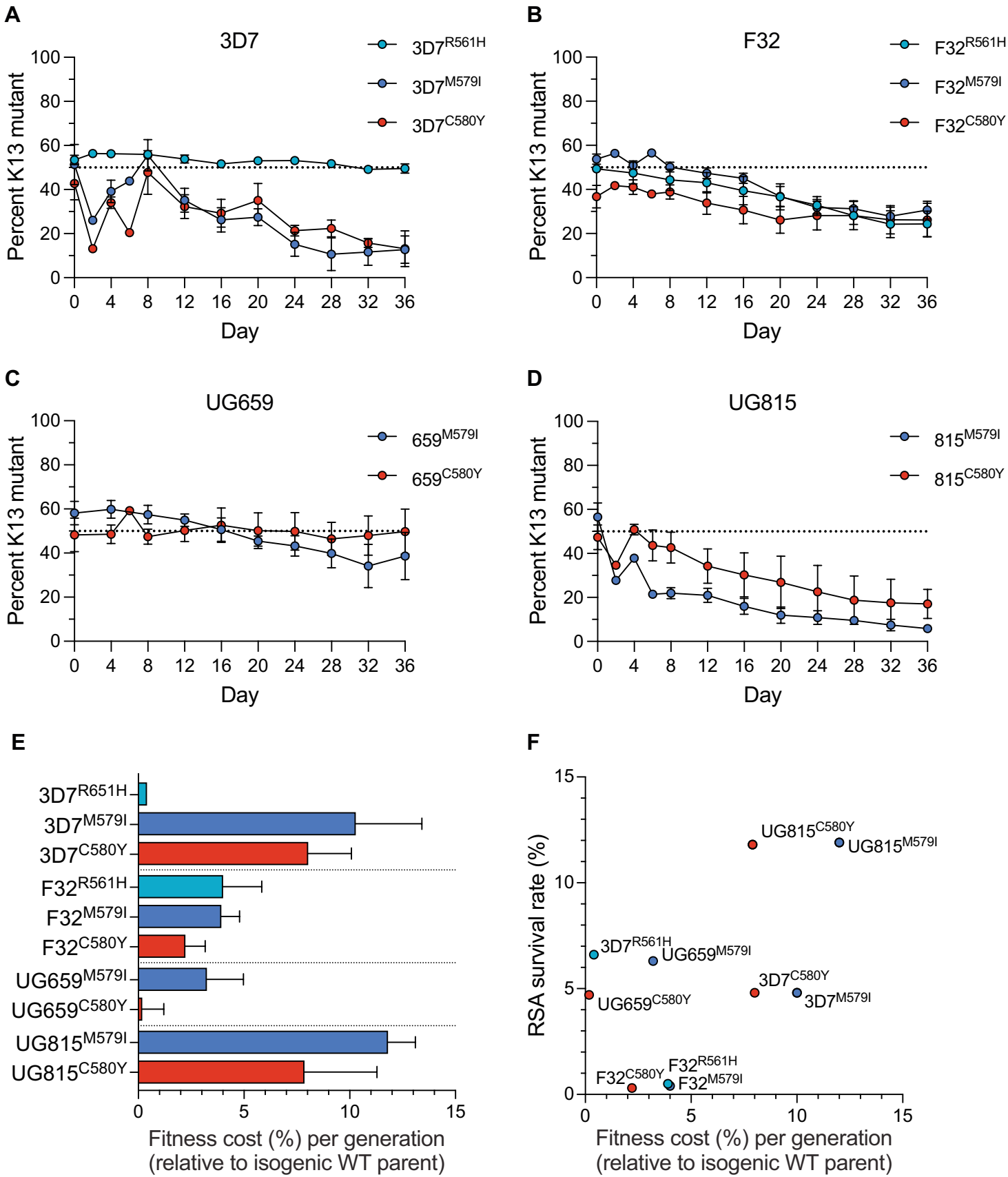
A
3D7
3D7R561H
3D7M579I
3D7C580Y
Percent K13 mutant
Day
B
F32
F32R561H
F32M579I
F32C580Y
Percent K13 mutant
Day
C
UG659
659M579I
659C580Y
Percent K13 mutant
Day
D
UG815
815M579I
815C580Y
Percent K13 mutant
Day
E
3D7R651H
3D7M579I
3D7C580Y
F32R561H
F32M579I
F32C580Y
UG659M579I
UG659C580Y
UG815M579I
UG815C580Y
Fitness cost (%) per generation
(relative to isogenic WT parent)
F
RSA survival rate (%)
UG815C580Y
UG815M579I
3D7R561H
UG659M579I
3D7C580Y
3D7M579I
UG659C580Y
F32C580Y
F32R561H
F32M579I
Fitness cost (%) per generation
(relative to isogenic WT parent)

Figure 4

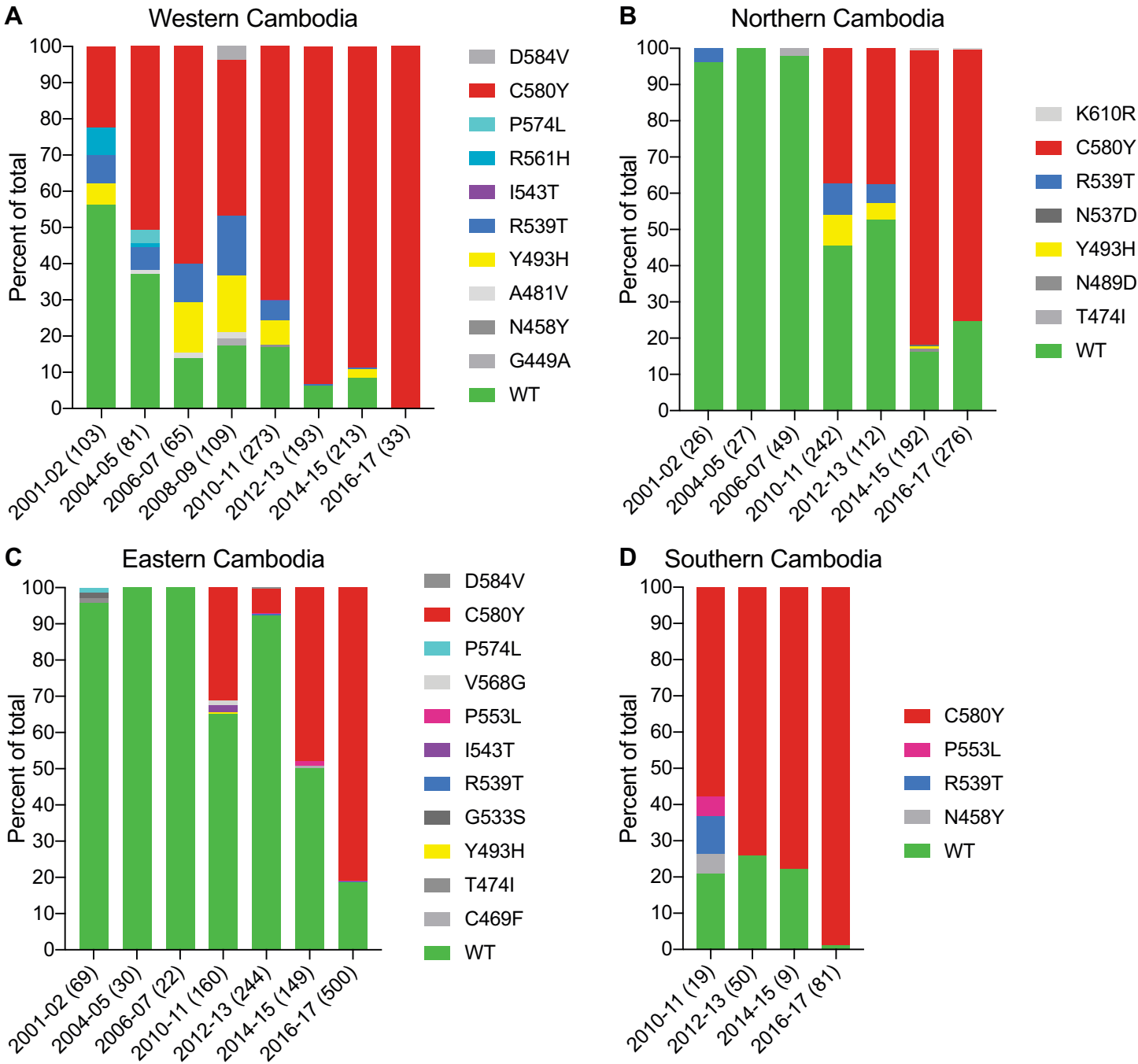
A
Western Cambodia
Percent of total
100
90
80
70
60
50
40
30
20
10
0
2001-02 (103)
2004-05 (81)
2006-07 (65)
2008-09 (109)
2010-11 (273)
2012-13 (193)
2014-15 (213)
2016-17 (33)
D584V
C580Y
P574L
R561H
I543T
R539T
Y493H
A481V
N458Y
G449A
WT
B
Northern Cambodia
Percent of total
2001-02 (26)
2004-05 (27)
2006-07 (49)
2010-11 (242)
2012-13 (112)
2014-15 (192)
2016-17 (276)
K610R
C580Y
R539T
N537D
Y493H
N489D
T474I
WT
C
Eastern Cambodia
Percent of total
2001-02 (69)
2004-05 (30)
2006-07 (22)
2010-11 (160)
2012-13 (244)
2014-15 (149)
2016-17 (500)
D584V
C580Y
P574L
V568G
P553L
I543T
R539T
G533S
Y493H
T474I
C469F
WT
D
Southern Cambodia
Percent of total
2010-11 (19)
2012-13 (50)
2014-15 (9)
2016-17 (81)
C580Y
P553L
R539T
N458Y
WT

Figure 5

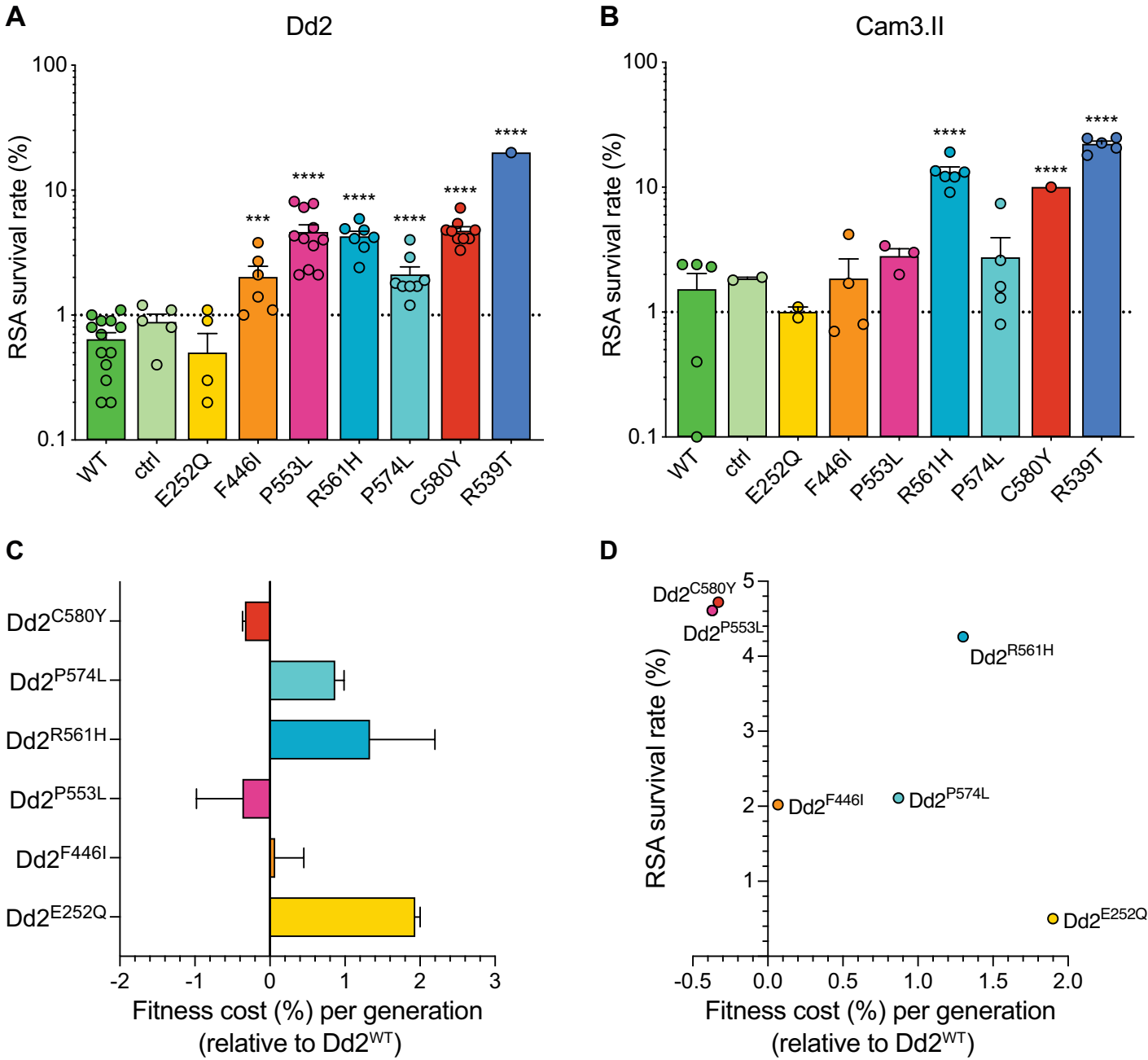
A
Dd2
RSA survival rate (%)
100
10
1
0.1
***
****
WT
ctrl
E252Q
F446I
P553L
R561H
P574L
C580Y
R539T
B
Cam3.II
C
Dd2C580Y
Dd2P574L
Dd2R561H
Dd2P553L
Dd2F446I
Dd2E252Q
-2
-1
0
1
2
3
Fitness cost (%) per generation
(relative to Dd2WT)
D
RSA survival rate (%)
5
4
3
2
1
-0.5
0.0
0.5
1.0
1.5
2.0
Fitness cost (%) per generation
(relative to Dd2WT)

Figure 6

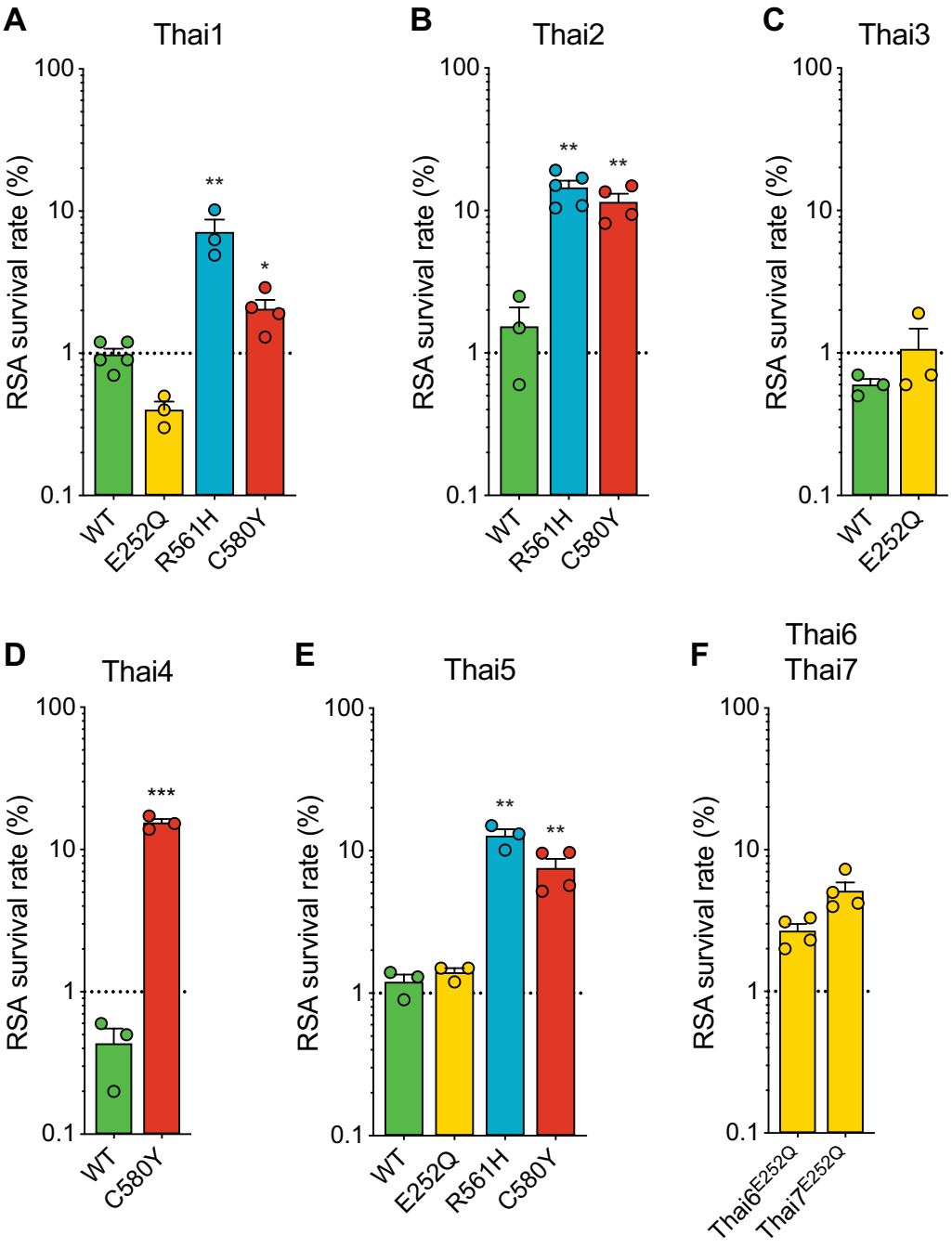
A
Thai1
B
Thai2
C
Thai3
D
Thai4
E
Thai5
F
Thai6
Thai7
RSA survival rate (%)
100
10
1
0.1
WT
E252Q
R561H
C580Y
Thai6E252Q
Thai7E252Q

Figure 7

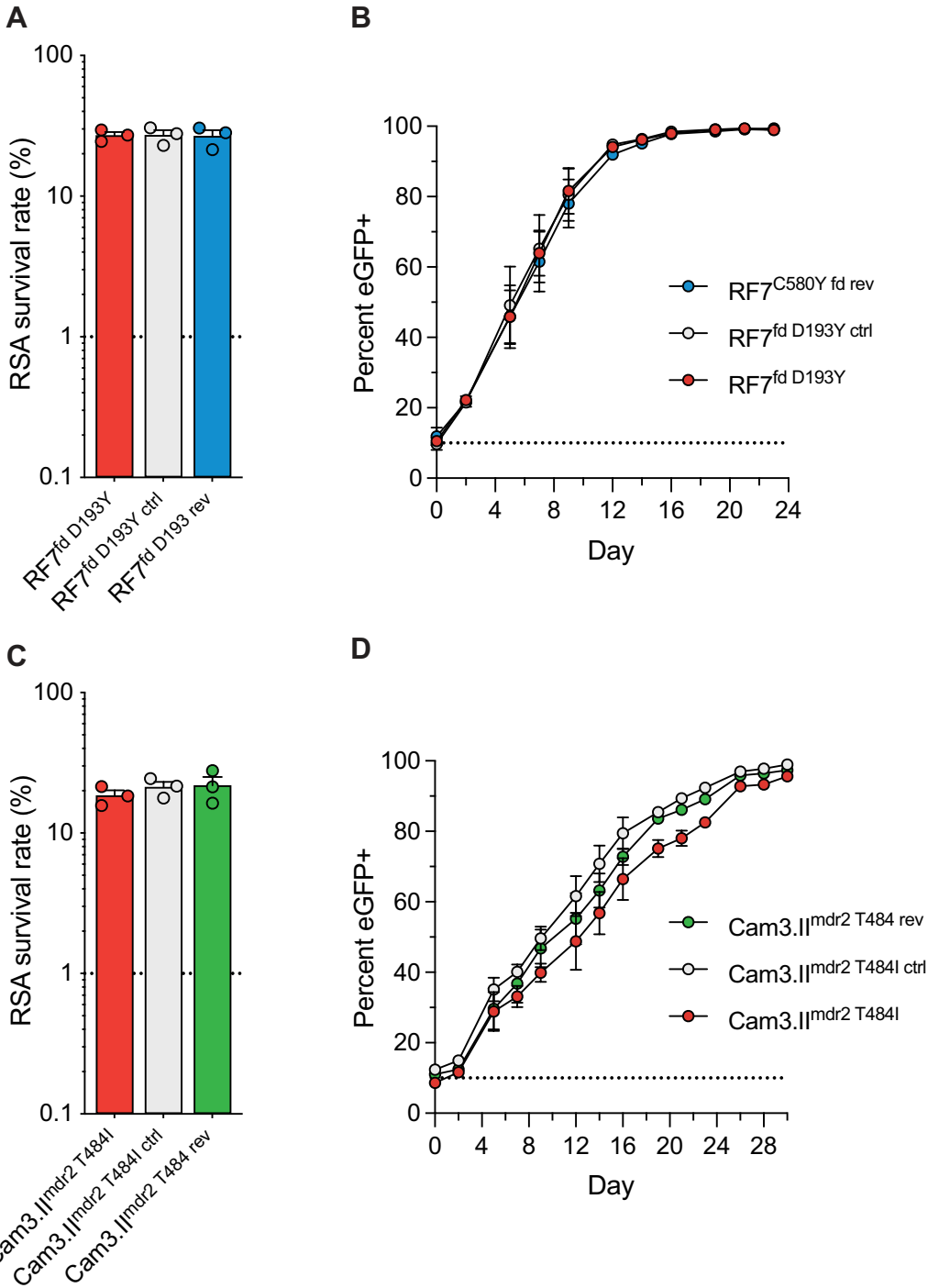
A
100
10
1
0.1
RSA survival rate (%)
RF7fd D193Y
RF7fd D193Y ctrl
RF7fd D193 rev
B
Percent eGFP+
Day
RF7C580Y fd rev
RF7fd D193Y ctrl
RF7fd D193Y
C
RSA survival rate (%)
Cam3.IImdr2 T484I
Cam3.IImdr2 T484I ctrl
Cam3.IImdr2 T484 rev
D
Percent eGFP+
Day
Cam3.IImdr2 T484 rev
Cam3.IImdr2 T484I ctrl
Cam3.IImdr2 T484I

Figure 2–figure supplement 1

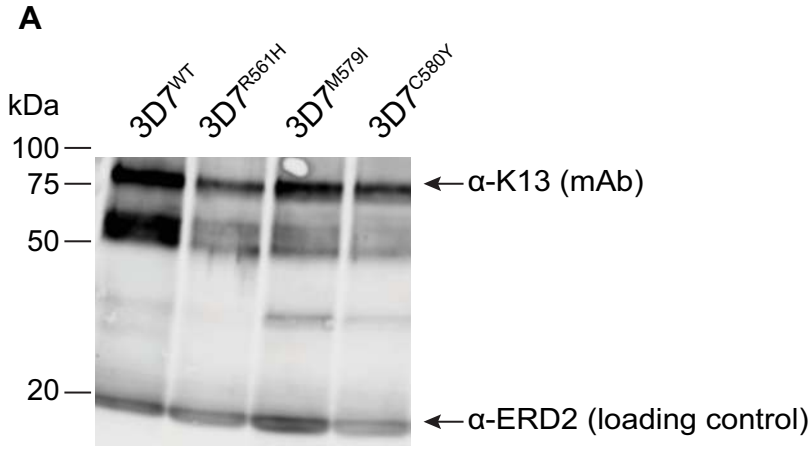

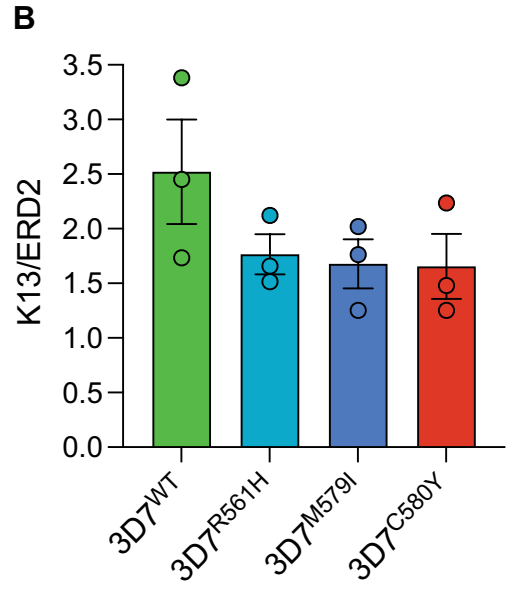

Figure 4–figure supplement 1

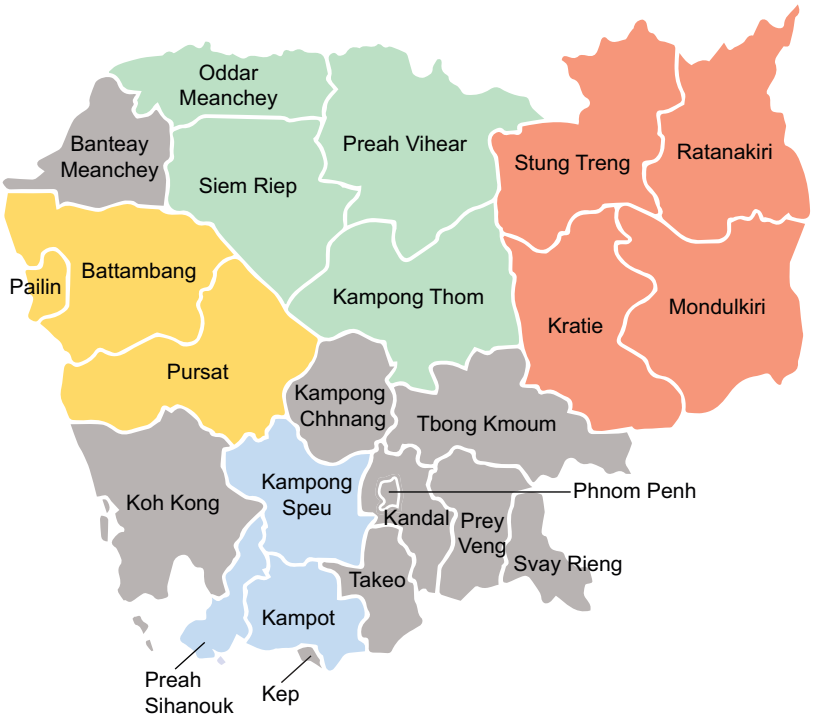

Western Cambodia
Battambang
Pailin
Pursat

Northern Cambodia
Oddar Meanchey
Preah Vihear
Kampong Thom
Siem Riep

Eastern Cambodia
Stung Treng
Ratanakiri
Mondulkiri
Kratie

Southern Cambodia
Kampong Speu
Kampot
Preah Sihanouk

Figure 5–figure supplement 1

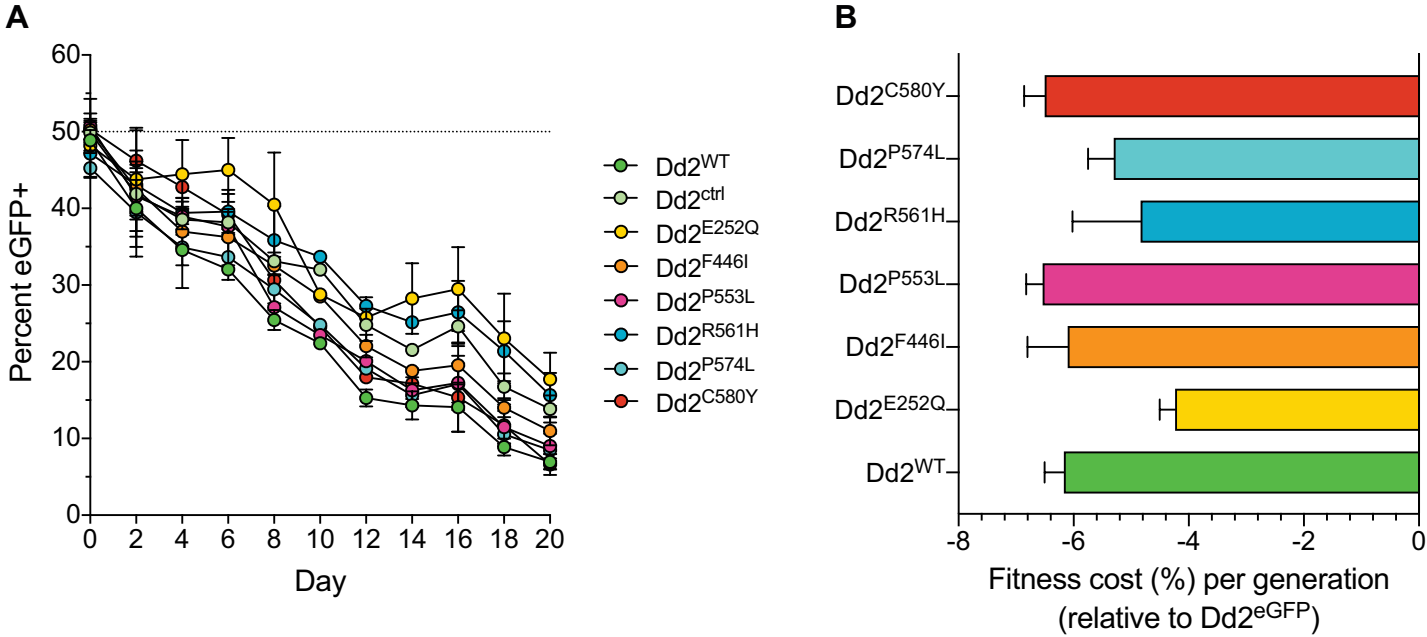

Figure 7–figure supplement 1